Journal of Medicinal Chemistry

Article

Synthesis and evaluation of new Hsp90 inhibitors based on a 1,4,5-trisubstituted 1,2,3-triazole scaffold

Maurizio Taddei, Serena Ferrini, Luca Giannotti, Massimo Corsi, Fabrizio Manetti, Giuseppe Giannini, Loredana Vesci, Ferdinando M. Milazzo, Domenico Alloatti, Mario B. Guglielmi, Massimo Castorina, Maria L. Cervoni, Marcella Barbarino, Rosanna Foderà, Valeria Carollo, Claudio Pisano, Silvia Armaroli, and Walter Cabri

J. Med. Chem., **Just Accepted Manuscript** • DOI: 10.1021/jm401536b • Publication Date (Web): 03 Mar 2014

Just Accepted

Journal of Medicinal Chemistry is published by the American Chemical Society. 1155 Sixteenth Street N.W., Washington, DC 20036

Synthesis and evaluation of new Hsp90 inhibitors based on a 1,4,5-trisubstituted 1,2,3-triazole scaffold.

Maurizio Taddei,[a*] *Serena Ferrini,*[a] *Luca Giannotti,*[a] *Massimo Corsi,*[a3] *Fabrizio Manetti,*[a] *Giuseppe Giannini,*[b*] *Loredana Vesci,*[b] *Ferdinando M. Milazzo,*[b] *Domenico Alloatti,*[b] *Mario B.Guglielmi,*[b] *Massimo Castorina,*[b] *Maria L. Cervoni,*[b] *Marcella Barbarino,*[b] *Rosanna Foderà,*[b] *Valeria Carollo,*[b] *Claudio Pisano,*[b1] *Silvia Armaroli*[c] *Walter Cabri.*[b2]

[a]Dipartimento di Biotecnologie, Chimica e Farmacia, Università degli Studi di Siena, Via A. Moro 2, I-53100 Siena, Italy.

[b]R&D Sigma-Tau Industrie Farmaceutiche Riunite S.p.A., Via Pontina Km 30,400, I-00040, Pomezia, Roma, Italy.

[c]Sigma-Tau Research Switzerland S.A., Via Motta, 2a, CH-6850 Mendrisio-Stazione, Switzerland.

[b1], [b2] and [a3]**:** see below Present Addresses

Abstract:

Ruthenium catalyzed 1,3-cycloaddition (click chemistry) of an azido moiety installed on dihydroxycumene scaffold with differently substituted aryl propiolates, gave a new family of 1,4,5-trisubstitued triazole carboxylic acid derivatives that showed high affinity towards Hsp90 associated with cell proliferation inhibition, both in nanomolar range. The 1,5 arrangement of the resorcinol, the aryl moieties, and the presence of an alkyl (secondary) amide in position 4 of the triazole ring, were essential to get high activity. Docking simulations suggested that the triazoles penetrate the Hsp90 ATP binding site. Some 1,4,5-trisubstitued triazole carboxamides induced dramatic depletion of the examined client proteins and a very strong increase in the expression levels of the chaperone Hsp70. *In vitro* metabolic stability and *in vivo* preliminary studies on selected compounds have shown promising results comparable to the potent Hsp90 inhibitor NVP-AUY922. One of them, (compound **18;** SST0287CL1) was selected for further investigation as the most promising drug candidate.

Introduction

Heat shock protein 90 (Hsp90) is an ubiquitous and abundant ATP-dependent molecular chaperone representing about 1-2% of the whole cytosolic proteomic load,[1] increasing up to ~ 4-6%. under stress conditions.[2] Hsp90 is a protein highly conserved from bacteria to mammals and it is documented to interact with more than 200 different "client" proteins involved in signal transduction, protein trafficking, receptor maturation and innate and adaptive immunity.[3-4] The main Hsp90 role is to promote the protein folding and the late-stage of maturation. Most of the so-called oncoproteins are Hsp90 clients.[4] Consequently, Hsp90 has emerged as an interesting molecular target for developing new anticancer agents, against several solid and hematological malignancies as well as towards leukemia stem cells.[5] Moreover, up-regulation of Hsp90 in several solid tumors likely unveils a "protective" role in tumorigenesis, thus confirming the key role of this chaperone protein in cancer cell growth and survival.[6] Besides, recent findings suggest a connection

between Hsp90 and cytotoxic drug resistance.[7-8] Finally, Hsp90 would seem also to have higher affinity toward small-molecule inhibitors in tumor cells than in normal cells.[9] Taken together, all these data point out Hsp90 as an attractive therapeutic target for cancer.[10] Although the target has been validated using the natural products geldanamycin and radicicol (Figure 1), to date there are no FDA approved Hsp90-targeting agents for human use. Currently, more than ten Hsp90 inhibitors are in different stages of clinical trials and an impressive growth in scientific and patent literature confirms the great interest toward this pharmacologic target from the academic and the pharmaceutical industry.[11]

Hsp90 inhibitor activity is mainly promoted by a competition with ATP binding to the N-terminus of the protein, although some inhibitors act through a non-competitive mechanism.[12] Most of the drugs actually in clinical trials are active through the ATP-competitive mechanism and some recent reviews collect most of the information on these molecules.[10,13-14] However, regardless of the chemical scaffolds, the new Hsp90 inhibitors have benefited greatly from structure-based design using available X-ray co-crystal structures[15] of different molecules bound to the N-terminal domain of Hsp90, associated to innovative approaches like high-throughput screening, fragment-based screening and virtual screening.[14] Despite the numerous efforts in developing new antitumor agents with Hsp90 inhibitory properties, the drugs currently under clinical investigation still show some critical limitations.[11] Therefore a medical need in this field is still felt.

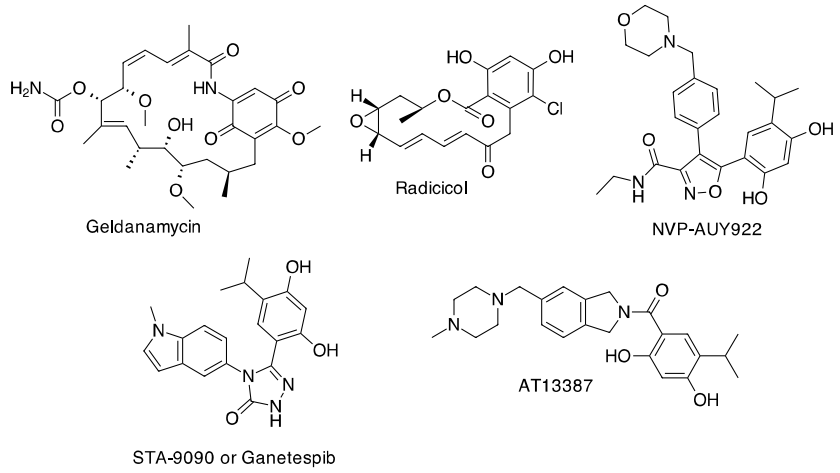

Figure 1. Some selective Hsp90 inhibitors.

In continuation of our interest in discovering new antitumor compounds,[16-18] we explored a new series of potential Hsp90 inhibitors having a 1,2,3-triazole scaffold. Although well-known in medicinal chemistry as a scaffold or a linker for diverse bio-medical applications, 1,2,3-triazoles have never been investigated as core structures of heterocycles Hsp90 inhibitors. This fact is even more surprising since parent heterocycles such as isoxazole,[19] 1,2,3-thiadiazole,[20] or 1,2,4 triazoles[21,22] have been very successful in targeting the ATP binding site of Hsp90.

After a preliminary exploration of the influence of substituent arrangement around the heterocycle on the activity as Hsp90 inhibitor, we report here the selective synthesis of various 1,4,5 trisubstituted 1,2,3-triazoles and their complete characterization as potent Hsp90 inhibitors with promising results in terms of metabolic stability and in vivo activity. From previous work on inhibitors of the Hsp90 ATP binding site,[19] it is known that the presence of a resorcinol-like fragment is extremely important to drive the binding mode and to get a strong interaction with the enzyme. One of the resorcinol hydroxyl groups displaces one water molecule required for substrate binding in the ATP region, while the other phenolic group contributes to an hydrogen bond network with the Asp93 residue. Starting from preliminary computational fitting experiments of different

triazole-based molecules on the Hsp90 X-ray structure,[18] we decided to keep the resorcinol fragment in position 1 of the triazole and explore the substitution pattern at positions 4 and 5.

Chemistry

Since 1,2,3-triazoles are suitably prepared by metal catalyzed [3+2] cycloaddition of azides and alkynes, the preparation of aryl azide **1** was required. This novel molecule was prepared as described in Scheme 1, starting from 2,4-dihydroxyacetophenone that was first protected as dibenzyl ether and then transformed[19] into alkene **2**.

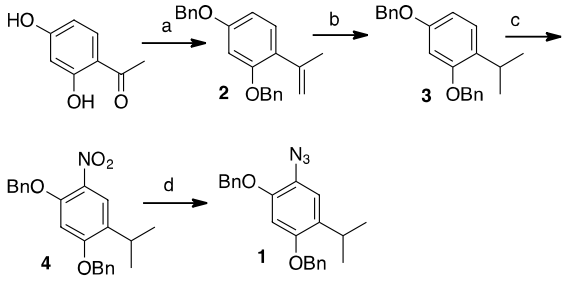

Scheme 1a) BnBr, K_2CO_3, MeCN followed by $MePPh_3Br$, BuLi THF, see ref. 19. b) H_2 (1 Atm) Pd/C EtOH rt 6h followed by BnBr, K_2CO_3, MeCN reflux, 3 h (94% overall). c) HNO_3 conc, AcOH, 70 °C, 30 min. (35%)d) i: $SnCl_2$, HCl, EtOH, 80 °C, 3 h; ii: *t*-BuONO, Me_3SiN_3, MeCN, rt, 12 h (75% over two steps).

Subsequent reduction followed by an additional step of benzylation of the phenolic OH (deprotected during reduction) gave compound **3**. The latter was selectively nitrated to give **4** which was then reduced and treated with $TMSN_3$ in the presence of *t*-butylnitrite to give the required azide **1** in good yield (75%). Azide **1** was submitted to Cu(II) catalyzed cycloaddition with phenylacetylene derivative **5** giving compound **6** as a single regioisomer although in moderate yields (Scheme 2). The other regioisomer **7** was obtained via Ru catalysis $(Cp^*RuCl)_4$ in good yields.

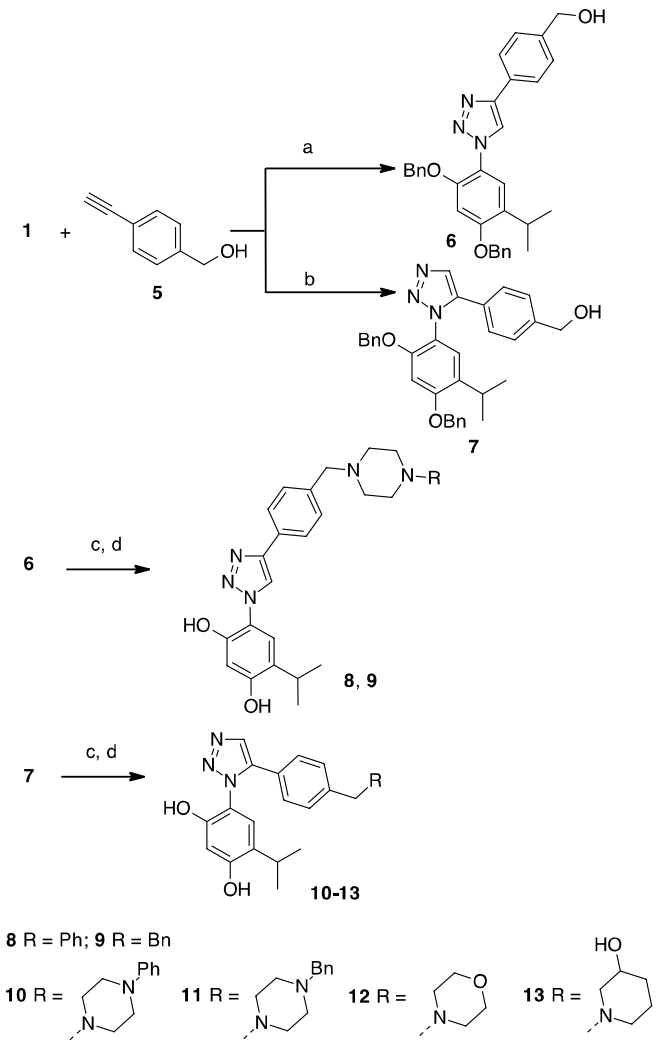

Scheme 2 a) $CuSO_4$, Na-ascorbate, DMF, rt, 12 h (55%). b) $(Cp^*RuCl)_4$ DMF; rt, 3 h (72 %) c) i: MsCl, TEA, DCM, rt, 2-4 h. ii: amine, DMF, Et_3N, rt, 12 h. d) BCl_3, DCM, 0° C to rt, 2 h.

Alcohols **6** and **7** were therefore transformed into their corresponding mesylates which were submitted to nucleophilic displacement with N-phenyl or N-benzyl piperidine. After the last removal of the phenolic benzyl protection, compounds **8-9** and **10-11** (Scheme 2) were isolated in 65-85 % yield and analysed in an Hsp90 binding assay. Since the 1,5 disubstituted regioisomers appeared to be more active compounds than the corresponding 1,4 disubstitued triazoles (see Table 1), two alternative fragments were introduced in position 5 following the same synthetic procedure. Resulting compounds **12** and **13** showed even more encouraging Hsp90 binding properties in two-digit nanomolar range (see Table 1) confirming that the 1,5 arrangement around the 1,2,3-triazole ring was more profitable than 1,4 arrangement. However, the activity of compounds **10-13** against a

selected panel of cancer cells was poor. Following experiences previously described in the literature,[18,19] a carboxyamide was introduced in position 4. This kind of arrangement (1-aryl, 5-aryl, 4-carboxy, 1,2,3-triazole) has been scarcely studied and only few examples of regiocontrolled preparation of trisubstituted 1,2,3-triazoles have been described in the literature.[23,24] Alkyne **5** was protected with TBDMSCl and, after deprotonation with LiHDMS, coupled with methylchloroformate to give compound **14** in good yields, the latter being the key intermediate toward the synthesis of the carboxamide variants of **10-13** (Scheme 3).

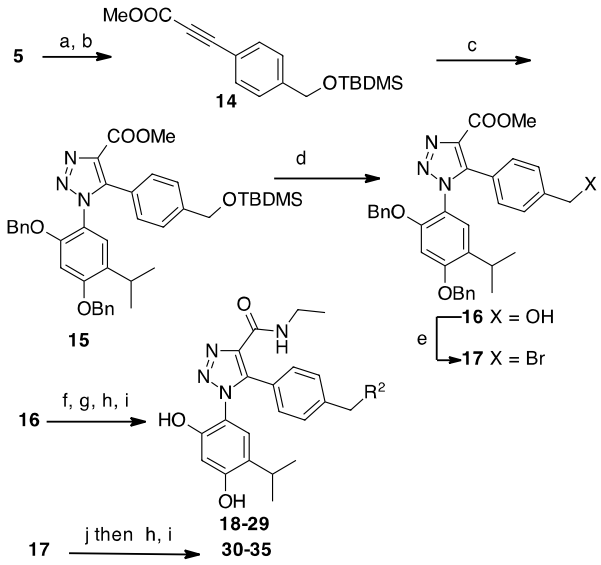

Scheme 3 a) TBDMSCl, Imidazole, DMF, rt, 12 h. b) LiHDMS, MeOCOCl, THF, -78 °C (76% over two steps). c) $(Cp^*RuCl)_4$ DMF, rt, 12 h, (68 %). d) TBAF, THF, rt, 2 h (80 %). e) CBr_4, PPh_3, DCM, rt, 3 h (87 %). f) MsCl, Et_3N, DCM, 0 °C then rt for 12 h (90% crude). g) Secondary amine, Et_3N, DMF, rt. h) Ethyl amine, MeOH 80 °C, 48 h. i) H_2 (1 Atm) $Pd(OH)_2$ cat., 4 h rt. j) Primary amine Et_3N, DMF, rt.

In fact, the Ru catalyzed cycloaddition of **14** with azide **1** proceeded with complete regioselectivity giving exclusively the isomer with the -COOMe opposite to the residue coming from the azide (compound **15** in Scheme 3). The coordination between the carboxylate and the Ru probably makes it as the most hindered group, orienting consequently the transition state towards compound **15**. Removal of the TBDMS group gave alcohol **16** that, after transformation into the corresponding mesylate, was submitted to reaction with different secondary amines that gave the expected mesylate displacement. After a further transformation of the methylcarboxylate in position

4 into ethylamide and removal of the benzylic protection, compounds **18-29** (entries 2-15 in Table 2) were obtained in good yields. However, when the reaction between the mesylate derived from**16** and a primary amine was attempted, the corresponding secondary amines were isolated in very poor yield. Thus the procedure was slightly modified, transforming first the benzyl alcohol **16** into the corresponding benzyl bromide **17**. On this substrate, the nucleophilic displacement with the primary amines worked well and, after the synthetic sequence outlined above, compounds **30-35** (entries 16-21 in Table 2) were isolated in acceptable overall yields. With the aim of also exploring the influence of different substituents in position 4, morpholine was introduced on alcohol **16** and the corresponding methylcarboxylate **36** reacted with different amines to give, after phenolic hydroxyl group deprotection, amides **37-43** (Scheme 4 and entries 22-28 in Table 2). Finally, in order to verify the possibility to get an active prodrug, compound **18** was acetylated to give **44** (Scheme 4).

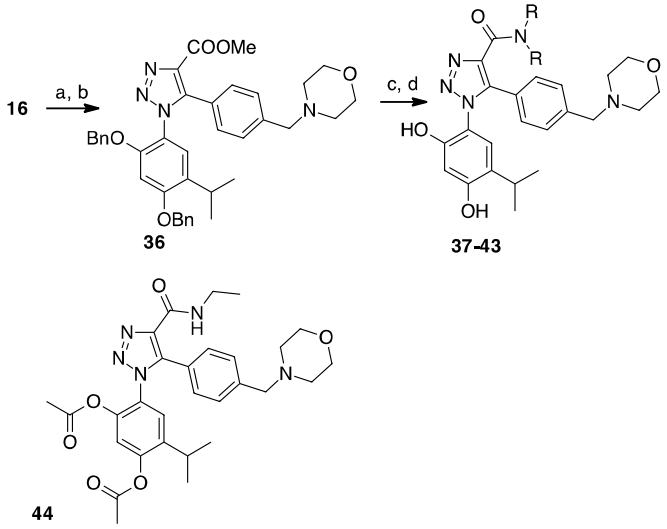

Scheme 4. a) MsCl, Et_3N, DCM, 0 °C then rt for 12 h b) Morpholine, Et_3N, DMF, rt, 12 h (75 % over two steps) c) i: LiOH in THF H_2O. ii: $(COCl)_2$ iii: primary or secondary amine. iv:BCl_3 in DCM, 0°C to rt (31 % over three steps).

Results and Discussion

We systematically investigated several molecules for their affinity to human Hsp90 and their antiproliferative activity on two tumor cell lines (NCI-H460 non-small cell lung carcinoma and A431 epidermoid carcinoma cells). As shown in Tables 1 and 2, all the compounds showed

appreciable binding to recombinant human Hsp90α protein in a fluorescence polarization (FP) assay, (see Note S1), with potency similar or even higher than NVP-AUY922, one of the most active reference compounds.[25] In general, tertiary amines showed better binding than secondary analogues, except in the case of the cyclohexylmethylamine containing derivatives **30** and **31** that retained a binding in the single-digit nanomolar concentration. Among tertiary amines, better results were obtained introducing a morpholine fragment (compound **18,** SST0287CL1), also present in the reference product. Analogously, piperazine derivatives **26-27** and the 4-amino substituted piperidine **28** have a high affinity with Hsp90. It is worth of note that the piperidine derivative **20** is at least four times less active than the corresponding morpholine or pirrolidine containing compounds **18** and **21**. Analogously, the presence of an aliphatic cycle in position 5 of the triazole is not mandatory for the activity if a second polar group is present (compare **25** and **18**). Regarding position 4, some variations of the substitution pattern are tolerated. The introduction of groups with more than 4 atoms (**38**) or with different functional group (**37**) causes only a partial reduction in the binding (33 and 17 nM, respectively). A significantly lower affinity is found when a cyclic substituent (**39**-**41**) or a branched side chain (**42**) is introduced. Although the presence of a substituted carboxamide is indispensable to get an acceptable level of cytotoxicity, the influence of the substituent nature on this property was more difficult to rationalize. Finally, while acetylation of the OH prevents the binding to Hsp90 (>1,000 nM), the cytotoxicity of **44** is still comparable with that of the parent compound **18** (6.5 vs. 4 nM, respectively), suggesting the possibility to intervene on this part of the molecule in order to improve the pharmacokinetic profile of the product.[26]

The cytotoxicity activity of some compounds of the series was comparable to that of the reference product NVP-AUY922 although they showed higher affinity to Hsp90 due to the many variables associates to a complex system such as a cell. In particular, **18**, **21**, and **31** were active toward NCI-H460 cells at one-digit nanomolar concentration. This antiproliferative activity trend of 1,2,3-triazole derivatives was confirmed by results obtained on an extensive panel of tumor cell lines, by means of a sulphorhodamine B (SRB) colorimetric test. The most active derivatives inhibited

growth of all tumor cell lines evaluated irrespective of cancer types or genetics (see Table S1). Tumor cell lines were selected based on their peculiar genotype, with particular attention to expression of key wild type or mutated Hsp90 client proteins, or with the aim of covering a wide array of tumor types (see Table S1) .

In order to have a more precise picture of the interaction mode of our compounds with Hsp90, docking simulations were performed using the complex between the N-terminal domain of Hsp90α and NVP-AUY922 (PDB entry 2VCI) as a template. Energy minimization of the resulting docked complexes showed triazole derivatives in an orientation almost identical to that of the reference inhibitor, with slight differences in the interaction pattern, the triazole N2 being involved in a water-bridged hydrogen bond with the carboxy terminus of Asp93.

The resorcinol hydroxyl group at position 2 shows both direct and water-mediated hydrogen bonds with the carboxyl terminus of Asp93. In a similar way, the second resorcinol hydroxyl group is involved in water-mediated hydrogen bonds with both the carboxyl terminus of Asp93 and hydroxyl group of Ser52. A direct hydrogen bond is also found between the Ser52 OH and the Asp93 carboxyl moiety. The isopropyl group of the inhibitor is embedded within a large hydrophobic cavity delimited by Leu48, Leu107, Thr109, Phe138, Val150, and Val186. The NH and CO portions of the C4 amide group are anchored by hydrogen bond interactions with the Gly97 carbonyl and the terminal ammonium group of Lys58, respectively, while the terminal ethyl chain of the ligand is exposed to solvent and shows lipophilic contact with the side chain of Ile96 (Figure 2).

A structural motif which significantly contributes to the stability of the complex is constituted by an additional network of charge-reinforced hydrogen bond interaction involving the protonable portion of the ligand (i.e., the basic nitrogen atom of morpholine, piperidine, pyrrolidine, and acyclic amino groups), the Asp54 carboxy terminus and the ammonium group of Lys58. The terminal portion of the substituent at C5, beyond the benzyl moiety and usually corresponding to a solubilizing functionality (such as morpholine, piperidine, pyrrolidine, etc.), is pointing toward solvent and does

not show any contact with the protein, apart the interaction between the protonated nitrogen (if present) and the carboxy terminus of Asp54. Depending on the terminal substituent, a different number of water molecules can be recruited.[27]

An analysis of molecular interactions between Hsp90 and **18** in comparison to those found in the crystallographic complex with AUY922 does not allow us to justify the difference in affinity measured between the two compounds. However, it should be pointed out that docking simulations and energy minimization performed on the Hsp90-**18** complex are based on a molecular mechanics approach (OPLS force fields) that is, by definition, almost unable to account for electronic contribution to binding. A quantum mechanics treatment of the interactions between Hsp90 and its inhibitors, that is not among the purposes of this work, is more appropriate to attempt to justify differences in activity. For example, HOMO and LUMO amplitude and their spatial location as well as dipole moment, are significantly different in triazoles in comparison to oxazole, thus suggesting a possibly different behavior toward a protein binding site.

The next step was to establish whether the new ligands retain the well-established molecular signature of known Hsp90 inhibitors, in terms of capacity to modulate cellular markers expression (client proteins). To this aim, the ability of selected compounds (i.e., **18**, **19**, **20**, **24**, **31**, **32**, **39** and **44**) to down-regulate the expression of representative Hsp90 client proteins and to induce the expression of Hsp70 protein was determined in the A431 (human squamous cell carcinoma) cell line (overexpressing EGFR). Western Blot analysis, after 24 hour exposure to several concentrations (dose-response curves) of selected test compounds, evidenced the expected depletion of the client proteins EGFR, CDK4, and Akt, as well as the induction of Hsp70 in a dose-dependent manner, thus confirming the efficacy of these compounds as novel potent Hsp90 inhibitors (Figures 3-4 and Figure S1).

According to the previous data, **18** appeared to have the most interesting profile, displaying ability to bind Hsp90 with an affinity comparable (or even better)[25] in respect to the reference compound, associated to a strong anti-proliferative activity. Furthermore, **18** caused dramatic depletion of

typical Hsp90 client proteins in A431 cells, associated to a very strong increase in the expression levels of the chaperone Hsp70, consistent with inhibition of Hsp90 function (Figure 4). In addition, as reported in Figure 4, the diacetyl derivative **44** displayed an extremely reduced ability to bind to recombinant Hsp90α in the FP assay, without significant changes in its antiproliferative efficacy, as a consequence of the Hsp90 chaperone inhibitory property of its putative metabolite (**18**), also confirmed by the impressive effect on depletion of client proteins and on increase of Hsp70 levels.

Flow cytometric analysis revealed that both **18** and NVP-AUY922 caused cell cycle arrest in G2/M upon treatment of NCI-H460 NSCLC cells, and a massive induction of apoptosis was triggered over the recovery times (Figure S2 and Table S2).

Subsequently, the antitumor efficacy of compounds **18** and **19** was evaluated in two tumor xenograft models (A431 epidermoid carcinoma and GTL-16 gastric carcinoma, overexpressing EGFR and c-Met, respectively). Both compounds, delivered intraperitoneally for 2 weeks according to the schedule q2d/wx2w or q4d/wx2w, were able to induce a significant tumor volume inhibition of about 40% ($P<0.05$). Moreover, the compounds showed to be well-tolerated since a little variation of body weight loss was found, except when the molecules were evaluated against GTL-16 which was a cachectic tumor xenograft (also the vehicle treated group revealed a significant body weight loss) (Table 3). The reference compound was evaluated at a higher dose according to the schedule qdx5/wx2w which was the maximum tolerated dose to investigate its efficacy (see Figures 5A, 5B, 5C). It is noteworthy that compounds **18** and **19** were administered at a total dose 6-10 fold lower than that used for NVP-AUY922. Its antitumor efficacy was lower than that found with **18** and **19** against A431 xenograft and comparable against GTL-16 tumor xenograft model, as shown in Figure 5**.**

To validate that the in vivo antitumor effect of test compounds was effectively related to the inhibition of Hsp90, the modulation of selected Hsp90 client proteins was assessed by Western Blot in tumor xenografts a few hours after the last treatment. As shown in Figure 6, **18** induced a very strong decrease in the protein levels of three typical client proteins (EGFR, Akt and Cdk4) in A431

tumor cell lysates and, at the same time, significantly increased the expression levels of the chaperone Hsp70, with a potency comparable with the reference compound (NVP-AUY922). Similar results were observed on the same animal model with compound **19** (data not shown).

The human gastric carcinoma cell line GTL-16 is characterized by the overexpression of c-Met (HGF receptor) protein, which is another key cellular protein tightly regulated by Hsp90.[28-29] For this reason, c-Met expression was also evaluated, instead of EGFR, in GTL-16 tumor xenografts in order to check the in vivo efficacy of **18** and **19**. Also in this animal model our compounds were shown to potently inhibit Hsp90, resulting in strong down-regulation of the selected client proteins and induction of Hsp70, with a similar behaviour compared to the reference compound (Figure 6).[30] In addition, our best candidate (**18**) showed a plasma stability comparable to that of the reference compound as showed by a quantitative LC/MS assay performed at 120 min (65 and 56%, respectively) (Table 4).

Finally, starting from the observation that a long chain residue installed on the amide did not significantly reduce the activity, a new derivative with a hydroxamic acid group on the hexamethylene chain was synthesized (compound **43** in Table 2). This group is a zinc binding group widely used in histone deacetylase (HDAC) inhibitors to coordinate the Zn ion located within the enzymatic site. The introduction of the HDAC binding arm fragment on a chemical structure already active on HSP90 did not reduce the binding activity too much (31 nM), although it was associated to a reduction of the cytotoxic activity (> 1 μM). On the other hand, **43** was also investigated as HDAC inhibitor on a panel of 10 isolated human HDAC isozymes (See SI). The assays were done in the presence of a fluorogenic peptide bound to the RHKK(Ac) fragment of p53 (residues 379-392), as the substrate, and using SAHA as the reference compound (Table 5).[31] Surprisingly, in addition to a good affinity to Hsp90, **43** demonstrated also a high selectivity towards the HDAC6 isoform. HDAC6 is predominantly a cytoplasmic, microtubule-associated member of the class IIB HDAC family, which is directly involved in controlling the HSP90 acetylation degree and function. Depletion of HDAC6 activity has been reported to affect HSP90

function in tumor cells.[32] These preliminary data support **43** as an interesting lead compound for further studies in the dual targeting HDAC/Hsp90 inhibition approach.

Conclusions

Among different 1,4,5-trisubstituted 1,2,3-triazole carboxamides prepared by regioselective Ru-catalyzed Huisgen reaction, the triazole scaffold carrying a resorcinol moiety in position 1, an ethylcarboxamide in position 4 and an arylmethylamine in position 5 demonstrated to have nanomolar binding to the N-terminus of Hsp90 and to induce cell death in different tumor cell lines. The antitumor activity of this class of compounds was demonstrated to proceed through Hsp90 inhibition, justified by a dramatic decrease in the levels of three typical client proteins (EGFR, Akt and Cdk4) in A431 cell lysates and, at the same time, a strong increment of expression levels of the chaperone Hsp70. Results of fluorescence activated cell sorting analysis, showed that compound **18** caused cell cycle arrest in G2/M upon treatment of NCI-H460 NSCLC cells, and that a massive induction of apoptosis was triggered over the recovery times. Several cancer cell lines resulted sensitive to different members of the class. Moreover, results of in vivo experiments carried out on different tumor xenograft models in mice showed that **18 (**SST0287CL1) induces a significant tumor volume inhibition and is well-tolerated, being active at a lower dose with respect to the reference compound. The diacetate derivative of the most active compound, maintaining a nanomolar cytotoxicity, suggests the possibility to modify this region of the structure to improve pharmacokinetic properties and bioavailability. These results point out that easily affordable 1,4,5-trisubstituted 1,2,3-triazoles are useful scaffolds to build new Hsp90 inhibitors (including potential HDAC / Hsp90 dual inhibitors). Further investigations are in progress to optimize the dose-activity profile of the compounds and to investigate this class of molecules in other therapeutic areas related to Hsp90 inhibition.

Experimental section

Animals. In vivo experiments were carried out using female athymic nude mice, 5-6 weeks old (Harlan). Mice were maintained in laminar flow rooms keeping temperature and humidity constant. Mice had free access to food and water. Experiments were approved by the Ethics Committee for Animal Experimentation of Sigma-Tau according to institutional guidelines.

Xenograft tumor model. For subcutaneous (s.c.) tumor model, exponentially growing tumor cells ($5x10^6$/100 µL) were s.c. inoculated in right flank of nude mice. Mice were treated starting three days after tumor injection. Tumor volume (TV) was measured biweekly and it was calculated according to the formula: TV (mm^3) = $d^2 \cdot D/2$ where d and D are the shortest and the longest diameter, respectively. The selected molecules were delivered intraperitoneally according to the schedule q2d/wx2w or q4d/wx2w. Drug efficacy was assessed as: (i) Tumor volume inhibition percentage (TVI%) in drug-treated versus control mice, expressed as: TVI% = 100 –[(mean TV treated/mean TV control)x100]. The day of TVI evaluation are reported in the Table 3. Toxic effects of the drug treatment were assessed as: (i) Body weight loss percentage (BWL%), calculated as: BWL% = 100- [(mean BW day x/mean BW day 1)x100], where day 1 was the first day of treatment and day x was any day thereafter. The highest (max) BWL% is reported in Table 3; (ii) Lethal toxicity, assessed as deaths occurring in treated mice before the death of the first control mouse.

The in vivo effect of selected inhibitors on the expression of typical Hsp90 client proteins was carried out by Western Blotting, as described in the section Client Protein Degradation Assay, on whole protein lysates that were prepared through homogenization of tumor samples (excised 2 h or 6 h after the last treatment) in T-PER tissue protein extraction reagent (Pierce, Rockland, IL, U.S.), supplemented with 10 μg/ml protease inhibitor cocktail (Sigma Chemical Co., St. Louis, MO, U.S.).

Cell lines and culture conditions. The A431epithelial carcinoma cell line (ATCC), the NCI-H460 non-small cell lung carcinoma cell line (ATCC), the ovarian carcinoma cell line A2780 (ECACC),

the MDA-MB436 breast carcinoma cell line (ATCC), the HeLa cervix uteri carcinoma cell line (Istituto Zooprofilattico di Brescia, I.) and the NB4 promyelocytic leukemia cell line (DSMZ) were routinely grown in RPMI-1640 medium (Lonza, Vierviers, B.), supplemented with 10% (v/v) heat-inactivated fetal bovine serum (GIBCO, Invitrogen, Paisley, UK). The GTL-16 gastric carcinoma cell line (kindly provided by Metheresis Translational Research S.A.) and the MiaPaCa2 pancreas carcinoma cell line (ECACC) were grown in DMEM (Lonza, Vierviers, B.), supplemented with 10% (v/v) heat-inactivated fetal bovine serum (GIBCO). The U87MG glioblastoma cell line (ATCC), the A498 renal carcinoma cell line (ATCC) and the MeWo melanoma cell line (ECACC) were grown in EMEM (Lonza, Vierviers, Belgium), supplemented with 10% (v/v) heat-inactivated fetal bovine serum (GIBCO). The HCT-116 colon carcinoma cell line (Istituto Zooprofilattico di Brescia) was grown in McCoy's 5A medium (Lonza, Vierviers, Belgium) , supplemented with 10% (v/v) heat-inactivated fetal bovine serum (GIBCO).

Cellular Sensitivity to Drugs. NCI-H460 non-small cell lung carcinoma and A431 epidermoid carcinoma cell lines were grown in a volume of 200 μL at approximately 10% confluence in 96-well-plates and were allowed to recover for an additional 24 h. Tumor cells were treated with either varying concentrations of drugs or solvent for 72 h. The fraction of cells surviving after compound treatment was determined using the SRB assay. IC_{50} values were defined as the drug concentration causing a 50% reduction in cell number compared with that of vehicle-treated cells and evaluated by the "ALLFIT" computer program by analyzing dose-response inhibition curves.

Binding on Hsp90 by a Fluorescence Polarization (FP) Assay. The ability of test compounds to compete with a fluorescently labelled probe for binding to full-length recombinant human Hsp90α (*cat. No. SPP-776* Stressgene, *VictoriaBC, Canada*) was determined by means of a suited fluorescence polarization assay, as previously described.[18] GM-FITC, supplied by *Invivogen (06C23-MT, California 92192, USA),* was used as probe. Fluorescence Polarization (FP) measurements were performed on a multi-label reader (*Wallac Envision 2101,Perkin Elmer, Zaventem, Belgium)*. Measurements were taken in Opti-Plate™-96F well plates *(Perkin Elmer,*

Zaventem, Belgium). The compounds were previously dissolved in DMSO and kept at -20 °C until use. The day of experiment, serial dilutions of stock solutions were prepared in assay buffer (HFB), containing 20 mM HEPES pH 7.3, 50 mM KCl, 5 mM $MgCl_2$, 20 mM Na_2MoO_4 and 0.01% NP40. Bovine gamma globulin (0.1 mg/mL) and 2 mM DTT were freshly added to the assay buffer immediately before use. Each assay was carried out by adding 50 μL of the GM-FTC solution (5 nM) to 30 nM of Hsp90, in the presence of 5 μL of the test compounds at increasing concentrations. The plates were shacked at 4 °C for 4 h, and then the FP values in mP (millipolarization units) were recorded. The IC_{50} values were calculated as the inhibitor concentration allowing displacement of 50% of the tracer, through nonlinear least-squares analyses and curve fitting using the *Prism GraphPad* software program (*GraphPad software, Inc., San Diego, CA).*

Client Protein Degradation Assay. Client protein degradation was determined by Western Blotting as previously described.[18] Twenty-four hours after seeding, A431 (human epidermoid carcinoma) cells were treated for 24 hours with test compounds at various concentrations (dose-response curve), depending on their relative potency, and then processed to obtain whole-cell extracts. 17-DMAG (at the concentration of 0.2 μM) was used as internal reference inhibitor. Following treatment, cells were rinsed twice with ice-cold PBS and then lysed in RIPA buffer supplemented with protease and phosphatase inhibitors. Protein concentration was determined by the Bradford Protein Assay (Thermo Scientific, Rockford, IL, USA). Equal amounts of total proteins were separated through SDS-PAGE and then blotted onto nitrocellulose membranes. Non-specific binding sites were blocked by incubation of the membranes with 5% non-fat dry milk in TBS, overnight at 4 °C. Membranes were finally probed with the following primary antibodies: anti-EGFR (Upstate Biotechnology, Millipore Corporate, Billerica, MA, USA), anti-Cdk4 (Santa Cruz Biotechnology Inc., CA, USA), anti-Akt (Cell Signaling Technology, Inc., MA, USA), anti-HSP70 (BRM-22) and anti-Actin (Sigma Chemical Co., St. Louis, MO, USA). After extensive washings in TBS-T, membranes were incubated with appropriate dilutions of a horseradish peroxidase-conjugated corresponding secondary antibody. Finally, immunoreactive bands were

detected by means of the ECL Plus detection system (GE Healthcare Bio-Sciences, Uppsala, Sweden), and acquired by a phosphorimaging system (STORM 860; Molecular Dynamics, Sunnyvale, CA).

Plasma Stability. Test compounds were added to human plasma to get a final concentration of 5 μM and incubated at 37 °C at different times (until 120 minutes). 0.1 mL of each sample was taken, added in a corresponding two-fold amount of chilled acetonitrile, centrifuged at +4 °C. The supernatant was then submitted to LC-MS/MS analysis. At the end of incubation, % of residual intact compound remaining was calculated.

Docking. The three-dimensional structure of Hsp90 in complex with a 4,5 diaryl isoxazole inhibitor derived from X-ray crystallography (pdb entry 2VCI, 2.0 Å resolution)[19] was used to create the initial coordinates for docking calculations. Protein Preparation Wizard (implemented within Maestro 9.2, Schroedinger, LCC) was used to prepare the protein structure, also adding hydrogen atoms and sampling water orientation. HOH2232, HOH2099, HOH2233, and HOH2115, that constitute a network of ordered and conserved water molecules, were kept for next calculations.

For preliminary fitting calculations of different triazole-based molecules on the Hsp90 ATP binding site,[18] inhibitor structures were prepared with LigPrep routine (implemented within Maestro 9.2, Schroedinger, LCC). Their conformations were generated by means of MacroModel, version 9.9 (Monte Carlo Multiple Minimum algorithm and an energy window of 10 kcal/mol), and docking calculations were performed with Glide (version 5.6). Final re-scoring of best poses was carried out with Prime 2.2, MM-GBSA routine.

Since Glide only modifies the torsional internal coordinates of the ligand during docking, without taking into account the remaining geometric parameters, we chose to apply a conformational search/energy minimization protocol to study the interaction between Hsp90 and the new triazole inhibitors. In particular, the structure of the co-crystallized isoxazole inhibitor was replaced by that of triazole derivatives (built with LigPrep) and the resulting complexes were submitted to a statistical conformational search (10000 steps of Statistical Pseudo Monte Carlo algorithm)

sampling all the rotatable bonds of the inhibitors. Moreover, the overall structure of the ligand was allowed to rotate and translate within the Hsp90 binding site. A continuum solvation approach was also applied, with the OPLS_2005 force fields and the Polak-Ribiere conjugate gradient algorithm for energy minimization (derivative convergence 0.01 kcal/Åmol). Only a substructure constituted by the inhibitor and a shell of amino acids within a 5 Å radius from the inhibitor was submitted to energy minimization, while keeping fixed the remaining part of the complex.

Chemistry. Reagents were purchased from commercial suppliers and used without further purification. General Remarks: ^{1}H-NMR spectra were recorded at the field frequency and in the solvent indicated. Peak positions are given in parts per million downfield from tetramethylsilane as the internal standard; J values are expressed in hertz. LC-MS analysis were recorded on a Waters Micromass ZQ-2000 instrument or on a double-focusing Finnigan MAT 95 instrument with BE geometry. Thin layer chromatographies (TLC) were carried out using Merck precoated silica gel F-254 plates. Flash chromatographies were done using Merck silica gel 60 (0.063-0.200 mm) using light petroleum (bp 40-60 °C) PE. Solvents were dried according to standard procedures and reactions requiring neutral atmosphere conditions were performed under argon. Solutions containing the final products were dried with Na_2SO_4, filtered and concentrated under reduced pressure using a rotatory evaporator. All the final products undergoing biological testing were >95% pure as demonstrated by analysis carried out with a Varian Prostar HPLC System equipped with an UV variable wavelength detector at 254 nm (column Gemini-NX C18 (150x4.8 mm, gradient A/B 95/5 to 50/50 in 15 min, A: 0.1 % formic acid in H_2O, B: 0.1% formic acid in acetonitrile, flow rate 1.5 mL/min, rt) .

2,4-Bis(benzyloxy)cumene (3). Pd/C (223 mg, 0.6 mmol) was added to a solution of **2** (4 g, 12.11 mmol)[17] in ethanol (40 ml) at rt and the mixture was hydrogenated (balloon, 1 atm) for 12 hours. The catalyst was filtered out through celite and the ethanol was removed under reduced pressure. The residue was dissolved in CH_3CN (25 mL) and K_2CO_3 (7.00 g, 50.6 mmol) was added. The

suspension was stirred for 15 min at rt. Benzyl bromide (5.49 ml, 50.6 mmol) was then added dropwise and the reaction mixture was refluxed for 3 hours. H_2O (40 mL) was added and the organic phase was extracted with EtOAc (3 x 30 mL). The organic phase was dried (Na_2SO_4) and the solvent removed. The title compound was obtained as a colourless solid (3.8 g, 94%). M.p. 76-78 °C. ^{1}H NMR (400 MHz, $CDCl_3$): δ 7.45-7.31 (m, 10 H), 7.11 (d, J = 8.4 Hz, 1 H), 6.60-6.53 (m, 2 H), 5.04 (s, 2 H), 5.02 (s, 2 H), 3.41-3.25 (m, 1 H), 1.21 (d, J = 6.8 Hz, 6 H).^{13}C NMR (100 MHz, $CDCl_3$): δ 157.9, 157.7, 136.6, 136.0, 129.2, 128.5, 128.4, 128.3, 127.9, 127.1, 126.6, 108.3, 102.3, 70.3, 70.0, 27.1, 23.3.

1- Nitro-2,4-bis(benzyloxy)cumene(4). HNO_3 (1.11 mL, 13.73 mmol) was added to a suspension of **3** (3.8 g, 11.44 mmol) in AcOH (46 mL) and the reaction was heated at 70°C for 30 min. The solution was cooled down to 0 °C and neutralized with aqueous $NaHCO_3$; the organic phase was extracted with EtOAc and the solvent was removed under reduced pressure. The crude was purified by flash chromatography (PE/EtOAc: 95/5 to 90/10) and the title compound was obtained as a yellow solid (1.51 g, 35%). M.p.: 89-90 °C. ^{1}H NMR (400 MHz, $CDCl_3$): δ 7.87 (s, 1 H), 7.43-7.31 (m, 10), 6.52 (s, 1 H), 5.14 (s, 2 H), 5.05 (s, 2 H), 3.30-3.23 (m, 1 H), 1.20 (d, J = 7.2 Hz, 6 H). ^{13}C NMR (100 MHz, $CDCl_3$): δ 160.1, 156.8, 138.3, 136.6, 134.8, 129.1, 128.4, 127.9, 126.6, 125.9, 124.6, 98.7, 72.1, 70.3, 26.5, 22.8.

1- Azido-2,4-bis(benzyloxy)cumene (1). $SnCl_2 \cdot 2\ H_2O$ (5.38 g, 23.85 mmol) and HCl (4.7 ml, 56.85 mmol) were added to a suspension of **4** (1.5 g, 3.98 mmol) in EtOH (38 mL). The reaction was heated at 80 °C for 3-4 hours; then it was cooled down to 0 °C and NaOH (28 ml of a 20% water solution) was added. The separated salts are filtered through celite and washed with EtOAc. The organic phase was extracted three times with EtOAc and the solvent was evaporated. To the residue (1.10 g, 3.18 mmol, 80%) dissolved inin CH_3CN (40 mL), *t*-BuONO (2.25 mL, 19 mmol) and $TMSN_3$ (2 ml, 15.2 mmol) were added and the mixture was stirred for 1 h at 0 °C and for 12 h at rt. The solvent was evaporated and the reaction crude was purified by flash chromatography

(PE/EtOAc: 95/5 to 90/10). The title compound was obtained as a brown waxy material (890 mg, 75%).^{1}H NMR (400 MHz, $CDCl_3$): δ 7.40-7.31 (m, 10 H), 6.82 (s, 1 H), 6.52 (s, 1 H), 5.04 (s, 2 H), 4.96 (s, 2 H), 3.31-3.24 (m, 1 H), 1.16 (d, J = 6.8 Hz, 6 H). ^{13}C NMR (100 MHz, $CDCl_3$): δ 157.8, 150.2, 139.3, 136.6, 132.6, 128.4, 127.8, 126.6, 125.6, 124.8, 117.7, 101.8, 70.3, 70.1, 26.3, 22.7. HRMS (ESI) calcd for $C_{23}H_{23}N_3O_2Na$ $(M+Na)^+$396.1688; found 396.1687.

1-[2,4-Bis(benzyloxy)cumenyl]-4-[*p*-(hydroxymethyl)phenyl]-1*H*-1,2,3-triazole (6). Azide **1** (100 mg, 0.27 mmol) was dissolved in DMF (1.5 mL) followed by (*p*-ethynylphenyl)methanol **5** (35 mg, 0.27 mmol) sodium ascorbate (5 mg, 0.027 mmol) and $CuSO_4.5H_2O$ (0.67 mg, 0.0027 mmol).The mixture was stirred at rt for 12 h. Water and EtOAc were added, the organic layer separated, dried over anhydrous $MgSO_4$ and the solvent evaporated. Column chromatography on silica gel (PE/EtOAc: 60/40) gave compound **6** as a waxy material (76 mg, 55%). ^{1}H NMR (400 MHz, $CDCl_3$): δ 7.63 (m, 2H), 7.40-7.22 (m, 12 H), 6.66 (s, 1H), 5.08 (s, 2H), 5.05 (s, 2H), 4.72 (s, 2H), 3.35 (qn, J = 7 Hz, 1 H), 2.25 (bs, 1H), 1.23 (d, 6 H, J = 7 Hz).^{13}C NMR (100 MHz, $CDCl_3$) δ 160.5, 156.4, 151.8, 142.5, 136.0, 135.9, 135.2, 128.7, 128.4, 128.0, 127.8, 127.6, 127.2, 126.5, 124.4, 123.8, 120.0, 112.1, 102.6, 70.1, 70.1, 64.2.

1-[2,4-Bis(benzyloxy)cumenyl]-5-[*p*-(hydroxymethyl)phenyl]-1*H*-1,2,3-triazole (7). Azide **1** (890 mg, 2.38 mmol) was dissolved in DMF (5 mL) and(*p*-ethynylphenyl)methanol **5** (286 mg, 2.16 mmol) was added at rt. The flask was subjected to three vacuum-nitrogen cycles, then $[Cp^*RuCl]_4$ (116 mg, 0.11 mmol) was added followed by other three vacuum-nitrogen cycles. The reaction was stirred at rt for 6 h. EtOAc (10 mL) and water (20 mL) were then added. The organic phase was extracted four times with EtOAc (10 mL), washed with water (three times) and brine (one time) and dried over Na_2SO_4; the solvent was removed and the mixture was purified by column chromatography (PE/EtOAc: 60/40). The title compound was obtained as a purple oil (866 mg, 72%).^{1}H NMR (400 MHz, $CDCl_3$): δ 7.85 (s, 1 H), 7.36-7.14 (m, 13 H), 6.87-6.83 (m, 2 H), 6.45 (s, 1 H), 4.97 (s, 2 H), 4.71 (s, 2 H), 4.69 (s, 2 H), 3.32 (qn, J = 6.8 Hz, 1 H), 1.21 (d, 6 H, J = 6.8 Hz,). ^{13}C NMR (100 MHz, $CDCl_3$): δ 157.65, 151.46, 141.66, 139.27, 136.42, 136.09, 131.75,

130.62, 128.61, 128.37, 128.04, 127.83, 127.62, 127.11, 126.95, 126.69, 126.48, 125.84, 118.56, 99.08, 70.71, 70.31, 64.60, 26.44, 22.57.

4-(5-{*p*-[(4-Phenyl-1-piperazinyl)methyl]phenyl}-1*H*-1,2,3-triazol-1-yl)-1,3-cumenediol (10). **General procedure.** Et_3N (160 μL, 1.17 mmol) and MsCl (90 μL, 1.17 mmol) were added to a solution of **7** (200 mg, 0.39 mmol) in DCM (5 mL) at 0 °C. The solution was stirred for 30 minutes at 0 °C and for 12 hours at rt. The solvent was removed under reduced pressure and the reaction crude was dissolved in DMF (2-3 ml). 1-Phenyl-piperazine (189 mg, 1.17 mmol) and Et_3N (160 μL, 1.17 mmol) were added and the reaction was stirred for 12 hours at rt. The mixture was diluted with H_2O and EtOAc, the organic phase was extracted with EtOAc (4 x 30 mL) and washed with H_2O (2 x 30 mL) and with brine (2 x 30 ml). The solvent was evaporated and the reaction crude was purified by passing through a silica gel cartridge eluting with EtOAc. The fraction were collected and the solvent was removed. The residue obtained was dissolved in dry DCM (3 mL), cooled to 0 °C and BCl_3 (680 μL of a solution 1 M in DCM, 0.68 mmol) was added. The mixture was stirred for 2 h at rt, saturated aqueous solution of $NaHCO_3$ was added (until the pH became slightly basic) and the organic phase was extracted with DCM (3 x 10 mL), washed with H_2O and dried over Na_2SO_4. The solvent was removed under reduced pressure. The reaction crude was purified by column chromatography (DCM/MeOH: 90/10) and the title compound was obtained as a purple oil (157 mg 86%). ^{1}H NMR (400 MHz, DMSO-d6): δ 10.25 (bs, 1 H), 10.09 (bs, 1 H), 9.25 (s, 1 H), 7.44-7.35 (m, 6 H), 7.20-7.16 (m, 2 H), 6.90-6.88 (m, 2 H), 6.77-6.73 (m, 1 H), 6.51 (s, 1 H), 3.52 (s, 2 H), 3.15-3.07 (m, 5 H), 2.49-2.47 (m, 4 H), 1.09 (d, J = 6.8 Hz, 6 H). ^{13}C NMR (100 MHz, DMSO-d6) δ 150.2, 150.1, 149.9, 144.3, 138.5, 131.2, 130.1, 129.1, 127.0, 125.7, 122.2, 120.4, 120.3, 116.8, 105.6, 62.9, 53.7, 50.7, 25.3, 22.7. HRMS (ESI) calcd for $C_{28}H_{32}N_5O_2$ $(M+1)^+$ 470.2556; found 470.2554.

4-(4-{*p*-[(4-Phenyl-1-piperazinyl)methyl]phenyl}-1*H*-1,2,3-triazol-1-yl)-1,3-cumenediol (8). Column chromatography was carried out with (DCM/MeOH: 90/10). The title compound was

obtained as a dense gray oil (110 mg, 60%). ^{1}H NMR (400 MHz, DMSO-d6): δ 8.03 (bs, 2H), 7.84-7.04 (m, 6H), 7.06-6.61 (m, 4H), 6.67-6.19 (m, 2H), 3.52 (s, 2H), 3.46 - 2.88 (m, 5H), 2.83-2.12 (m, 4H).1.07 (d, J = 6.8 Hz, 6H). ^{13}C NMR (100 MHz, DMSO-d6) δ 155.7, 151.8, 151.2, 150.2, 140.3, 129.1, 128.1, 126.7, 126.4, 124.1, 122.1, 120.3, 120.0, 116.8, 113.5, 100.5, 62.8, 56.7, 51.4, 23.3, 20.7. HRMS (ESI) calcd for $C_{28}H_{32}N_5O_2$ $(M+1)^+$ 470.2556; found 470.2553.

4-(4-{*p*-[(4-Benzyl-1-piperazinyl)methyl]phenyl}-1*H*-1,2,3-triazol-1-yl)-1,3-cumenediol (9). Column chromatography was carried out with (DCM/MeOH: 90/10). The title compound was obtained as a purple oil (97 mg, 52%). ^{1}H NMR (400 MHz, DMSO-d6): δ 8.13 (bs, 2H), 7.77 - 7.06 (m, 10H), 6.56 (m 1H), 6.40 (s, 1H), 3.52 (s, 4H), 3.22(q, J = 7 Hz, 1H), 2.81-2.18 (m, 8H)1.11 (d, J = 7 Hz, 6 H).^{13}C NMR (100 MHz, DMSO-d6) δ 155.7, 151.8, 151.2, 140.6, 137.8, 129.2, 128.1, 128.1, 127.5, 126.7, 126.4, 124.1, 122.1, 120.0, 113.5, 100.5, 62.9, 62.7, 52.8, 51.5, 25.7, 21.4. HRMS (ESI) calcd for $C_{29}H_{34}N_5O_2$ $(M+1)^+$ 484.2713; found 484.2711.

4-(5-{*p*-[(4-Benzyl-1-piperazinyl)methyl]phenyl}-1*H*-1,2,3-triazol-1-yl)-1,3-cumenediol (11). Column chromatography was carried out with (DCM/MeOH: 90/10). The title compound was obtained as a purple oil (158 mg, 85%).^{1}H NMR (400 MHz, DMSO): δ 10.26 (bs, 1 H), 10.11 (bs, 1 H), 9.24 (s, 1 H), 7.43-7.29 (m, 10 H), 6.54 (s, 1 H), 3.48-3.31 (m, 6 H), 3.13-3.06 (m, 1 H), 2.42-2.32 (m, 6 H), 1.08 (d, J = 6.8 Hz, 6 H).^{13}C NMR (100 MHz, DMSO): δ150.1, 149.9, 144.3, 138.7, 137.8, 131.1, 130.1, 129.2, 128.1, 127.5, 127.0, 127.0, 125.7, 122.2, 120.4, 105.6, 62.9, 62.7, 52.8, 25.3, 22.7. HRMS (ESI) calcd for $C_{29}H_{34}N_5O_2$ $(M+1)^+$484.2713; found 484.2715.

4-(5-{*p*-[(1-Morpholyl)methyl]phenyl}-1*H*-1,2,3-triazol-1-yl)-1,3-cumenediol (12). Column chromatography was carried out with (DCM/MeOH: 95/5). The title compound was obtained as a purple oil (105 mg. 68%). ^{1}H NMR (400 MHz, MeOD): δ 8.92 (s, 1 H), 7.47 (s, 4 H), 7.20 (s, 1 H), 6.38 (s, 1 H), 4.90 (bs, 2 H), 3.82 (s, 2 H), 3.75-3.68 (m, 4 H), 3.25-3.12 (m, 1 H), 2.78-2.70 (m, 4 H), 1.15 (d, J = 6.8 Hz, 6 H). ^{13}C NMR (100 MHz, MeOD): δ 150.1, 149.9, 144.3, 138.0, 131.1,

130.1, 127.1, 126.8, 125.7, 122.2, 120.4, 105.6, 67.1, 63.2, 53.8, 25.3, 22.7. HRMS (ESI) calcd for $C_{22}H_{27}N_4O_3$ $(M+1)^+$395.2083; found 395.2080.

4-(5-{*p*-[(3-Hydroxy-1-piperazinyl)methyl]phenyl}-1*H*-1,2,3-triazol-1-yl)-1,3-cumenediol (13). Column chromatography was carried out with (DCM/MeOH: 90/10). The title compound was obtained as a purple oil (105 mg, 66%). ^{1}H NMR (400 MHz, MeOD): δ 8.93 (s, 1 H), 7.49 (s, 4 H), 7.21 (s, 1 H), 6.40 (s, 1 H), 4.88 (bs, 3 H), 3.90 (s, 2 H), 3.92-3.77 (m, 1 H), 3.24-3.12 (m, 1 H), 2.95-2.50 (m, 4 H), 1.90-1.40 (m, 4 H), 1.16 (d, J = 6.8 Hz, 6 H). ^{13}C NMR (100 MHz, MeOD): δ 150.1, 149.9, 144.3, 139.3, 131.1, 130.1, 127.2, 126.6, 125.7, 122.2, 120.4, 105.6, 66.9, 66.8, 61.6, 55.4, 33.3, 25.3, 23.3, 22.7. HRMS (ESI) calcd for $C_{23}H_{29}N_4O_3$ $(M+1)^+$409.2240; found 409.2237.

Methyl 3-[*p*-(*t*-butyldimethylsilyloxymethyl)phenyl]propiolate (14). LiHMDS (5.8 ml of a solution 1M in toluene, 5.8 mmol) was added to a solution of the *tert*-butyldimethylsilyl ether of **5** (820 mg, 3.33 mmol) in dry THF (28 mL) at -78 °C. The reaction mixture was slowly warmed up to -40 °C and left for 1 hour at this temperature. ClCOOMe (420 μL, 5.41 mmol) was dissolved in THF (9.6 mL) and cooled down to -40 °C; the mixture prepared before was added to this solution *via cannula* and the reaction was warmed up to rt. A saturated solution of NH_4Cl was added to the mixture reaction; the organic phase was extracted with EtOAc (3 x 20 ml) and dried. The solvent was removed under reduced pressure and the reaction crude was purified by column chromatography (PE/EtOAc 95:5). The title compound was obtained as yellow oil that solidify on standing (0.769 g, 76%). M.p. 56-58 °C. ^{1}H NMR (400 MHz, $CDCl_3$): δ 7.51 (d, J = 8.0 Hz, 2 H), 7.30 (d, J = 8.0 Hz, 2 H), 4.72 (s, 2 H), 3.79 (s, 3 H), 0.91 (s, 9 H), 0.07 (s, 6 H). ^{13}C NMR (100 MHz, $CDCl_3$): δ 154.0, 144.2, 132.5, 125.5, 117.4, 86.3, 79.7, 63.9, 52.2, 25.4, 17.9, -5.8.

Methyl 1-[2,4-bis(benzyloxy)cumenyl]-5-[*p*-(t-butyldimethylsilyloxymethyl)phenyl]-1*H*-1,2,3-triazole-4-carboxylate (15). Compound **14** (277 mg, 0.91 mmol) was added at rt to a solution of azide **1** (373 mg, 1 mmol), dissolved in DMF (2.5 mL). The flask was subjected to three vacuum-nitrogen cycles, then $[Cp^*RuCl]_4$ (49 mg, 0.045 mmol) was added and the reaction mixture was

purged again three times. The reaction was left at rt until completion (12 h, monitored by TLC). EtOAc (20 mL) and water (10 mL) were then added. The organic phase was extracted four times with EtOAc, washed with water (three times) and brine (one time) and dried over Na_2SO_4; the solvent was removed and the mixture was purified by column chromatography (PE/EtOAc: 60/40). The title compound was obtained as a purple oil (419 mg, 68%). ^{1}H NMR (400 MHz, $CDCl_3$): δ 7.31-7.16 (m, 13 H), 6.94 (d, J = 7.2 Hz, 2 H), 6.41 (s, 1 H), 4.92 (s, 2 H), 4.72 (s, 4 H), 3.82 (s, 3 H), 3.30-3.23 (m, 1 H), 1.13 (d, J = 6.8 Hz, 6 H), 0.93 (s, 9 H), 0.09 (s, 6 H). ^{13}C NMR (100 MHz, $CDCl_3$): δ 161.3, 157.47 151.2, 142.6, 136.0, 135.7, 135.1, 129.8, 129.4, 128.12 128.1, 127.6, 127.5, 126.7, 126.4, 125.6, 124.9, 124.1, 117.1, 98.5, 70.2, 69.9, 64.1, 51.4, 25.9, 25.5, 22.1, 17.97, -5.66. HRMS (ESI) calcd for $C_{40}H_{47}N_3O_5SiNa$ $(M+Na)^+$ 701.3217 (43.3%), 700.3183 (100%); found 701.3215 (43%), 700.3181 (100%).

Methyl 1-[2,4-bis(benzyloxy)cumenyl]-5-[*p*-(hydroxymethyl)phenyl]-1*H*-1,2,3-triazole-4-carboxylate (16). TBAF (270 mg, 1.25 mmol) was added to a solution of **15** (460 mg, 0.68 mmol) in THF (4 mL) and the reaction was stirred for 2 hours at rt. EtOAc (20 mL) was added and the organic phase was washed with a saturated solution of NH_4Cl and with H_2O. After drying over Na_2SO_4, the solvent was removed under reduced pressure and the reaction crude was purified by column chromatography (PE/EtOAc 40:60). The title compound was obtained as a purple oil (310 mg, 80%). ^{1}H NMR (400 MHz, $CDCl_3$): δ 7.29-7.15 (m, 13 H), 6.93 (d, J = 6.8 Hz, 2 H), 6.37 (s, 1 H), 4.89 (s, 2 H), 4.70 (s, 2 H), 4.62 (s, 2 H), 3.79 (s, 3 H), 3.31-3.18 (m, 1 H), 1.12 (d, J = 6.8 Hz, 6 H). ^{13}C NMR (100 MHz, $CDCl_3$): δ 161.35, 157.57, 151.25, 142.69, 142.59, 136.01, 135.64, 135.10, 129.92, 129.53, 128.27, 128.16, 127.70, 127.63, 126.78, 126.45, 125.74, 125.62, 124.30, 116.98, 98.40, 70.33, 69.91, 63.87, 51.66, 26.04, 22.20. HRMS (ESI) calcd for $C_{34}H_{33}N_3O_5Na$ $(M+Na)^+$ 587.2352 (36.8 %) 586.2318 (100 %); found 587.2350 (36.6 %) 586.2316 (100 %).

Methyl 1-[2,4-bis(benzyloxy)cumenyl]-5-[*p*-(bromomethyl)phenyl]-1*H*-1,2,3-triazole-4-carboxylate (17). Triphenylphosphine (1.45 g, 5.54 mmol) and carbon tetrabromide (1.84 g, 5.54 mmol) were added to a solution of alcohol **16** (2.4 g, 4.26 mmol) in dry DCM (48 mL) at 0 °C. The

mixture was stirred at this temperature for one hour, then the solvent was removed under reduced pressure and the residue was purified by column chromatography (PE/EtOAc: 70/30). The title compound was obtained as a purple oil (2.32 g, 87%). However, the crude product could be directly employed in the next step without any chromatographic purification. ^{1}H NMR (400 MHz, $CDCl_3$): δ 7.40-7.16 (m, 13 H), 7.08-6.99 (m, 2 H), 6.41 (s, 1 H), 4.96 (s, 2 H), 4.71 (s, 2 H), 4.44 (s, 2 H), 3.89 (s, 3 H), 3.32-3.20 (m, 1 H), 1.16 (d, J = 6.8 Hz, 6 H). ^{13}C NMR (100 MHz, $CDCl_3$): δ 161.2, 157.5, 151.0, 141.8, 138.6, 135.9, 135.6, 135.2, 130.1, 129.7, 128.6, 128.1, 127.6, 126.7, 126.4, 125.7, 125.5, 117.0, 98.5, 70.4, 69.9, 51.6, 32.3, 26.0, 22.1. HRMS (ESI) calcd for $C_{34}H_{32}BrN_3O_4Na$ $(M+Na)^+$ 650.1454 (97.5 %), 648.1474 (100 %); found 650.1452 (97 %), 648.1471 (100 %).

{1-[2,4-Dihydroxycumenyl]-5-[*p*-(4-morpholin-4-ylmethy)phenyl]-1*H*-1,2,3-triazol-4-yl}(ethylamino)formaldehyde(18). General procedure. Et_3N (230 μL, 1.65 mmol) and MsCl (130 μL, 1.65 mmol) were added to a solution of **16** (310 mg, 0.55 mmol) in DCM (7 mL) at 0 °C. The solution was stirred for 30 minutes at 0 °C and for 12 h at rt. The solvent was removed under reduced pressure and the reaction crude was dissolved in DMF (3-4 mL). Morpholine (143 mg, 1.65 mmol) and Et_3N (230 μL, 1.65 mmol) were added and the reaction was stirred for 12 hours at rt. The mixture was diluted with H_2O and EtOAc, the organic phase was extracted four times with EtOAc (4 x 30 mL) and washed with H_2O (2 x 30 mL) and brine (2 x 30 ml). The solvent was evaporated and $EtNH_2$ (1.5 ml of a solution 2 M in MeOH) was added to the crude reaction product. The mixture was heated for 24 hours at 80 °C in a sealed tube. The solvent and the excess of amine were removed under reduced pressure and the residue was dissolved in EtOH (5 ml) and $Pd(OH)_2/C$ (0.01 mmol) was added. The mixture was stirred under an atmosphere of hydrogen (balloon) for 1 hour. The catalyst was filtered off through celite and the ethanol was removed under reduced pressure. The reaction crude was purified by column chromatography (DCM/MeOH: 90/10). The title compound was obtained as a purple oil (174 mg, 68%). ^{1}H NMR (400 MHz, MeOD): δ 7.30-7.25 (m, 4 H), 6.82 (s, 1 H), 6.31 (s, 1 H), 4.84 (bs, 3 H), 3.63-3.61 (m, 4 H), 3.46

(s, 2 H), 3.37 (q, *J* = 7.2 Hz, 2 H), 3.10 (qn, *J* = 6.8 Hz, 1 H), 2.41-2.39 (m, 4 H), 1.19 (t, *J* = 7.2 Hz, 3 H), 1.03 (d, *J* = 6.8 Hz, 6 H). ^{13}C NMR (100 MHz, MeOD): δ 161.1, 156.6, 150.8, 140.0, 137.8, 137.4, 129.4, 128.1, 126.3, 125.1, 125.0, 114.4, 101.8, 65.8, 62.0, 52.7, 33.2, 25.5, 21.1, 13.2. HRMS (ESI) calcd for $C_{25}H_{32}N_5O_4$ $(M+1)^+$ 466.2454; found 466.2452.

Compound 19. Column chromatography with (DCM/MeOH: 90/10) gave compound **19** as a purple oil (166 mg, 63%). ^{1}H NMR (400 MHz, MeOD): δ 7.29 (*AB* system, *J* = 8.0 Hz, 4 H), 6.85 (s, 1 H), 6.33 (s, 1 H), 4.85 (bs, 3 H), 3.66-3.61 (m, 1 H), 3.51 (s, 2 H), 3.39 (q, *J* = 7.2 Hz, 2H), 3.11 (qn, *J* = 6.8 Hz, 1 H), 2.87-2.84 (m, 1 H), 2.64-2.61 (m, 1 H), 2.01-1.85 (m, 4H), 1.70-1.67 (m, 1 H), 1.54-1.44 (m, 1 H), 1.22 (t, *J* = 7.2 Hz, 3 H), 1.04 (d, *J* = 6.8 Hz, 6 H). ^{13}C NMR (400 MHz, MeOD): δ 161.1, 156.5, 150.8, 140.8, 137.9, 137.4, 129.3, 128.2, 126.3, 125.0, 114.4, 101.9, 65.9, 61.7, 59.8, 52.3, 33.2, 31.9, 25.5, 22.0, 21.1, 13.2. HRMS (ESI) calcd for $C_{26}H_{34}N_5O_4$ $(M+1)^+$ 80.2611; found 480.2608.

Compound (S-19) The product was isolated using (*S*)-3-hydroxypiperidine and following the same procedure as **19** (161 mg, 61 %). It showed the same spectroscopic features of **19**. $[a]^{25}_D$ = + 12.2 (c= 0.1 in MeOD).

Compound (*R*-19) The product was isolated using (*R*)-3-hydroxypiperidine and following the same procedure as **19**(146 mg, 55 %). It showed the same spectroscopic features of **19**. $[a]^{25}_D$ = -11.9 (c= 0.1 in MeOD).

Compound 20. Column chromatography with (DCM/MeOH: 90/10) gave compound **20** as a purple oil (165 mg, 65%). ^{1}H NMR (400 MHz, MeOD): δ 7.31 (*AB* system, *J* = 8.6 Hz, 4 H), 6.84 (s, 1 H), 6.33 (s, 1 H), 4.87 (bs, 3 H), 3.59 (s, 2 H), 3.39 (q, *J* = 7.2 Hz, 2 H), 3.10 (qn, *J* = 6.8 Hz, 1 H), 2.53-2.49 (m, 4 H), 1.61-1.57 (m, 4 H), 1.49-1.45 (m, 2 H), 1.21 (t, *J* = 7.2 Hz, 3 H), 1.06 (d, *J* = 6.8 Hz, 6 H). ^{13}C NMR (100 MHz, MeOD): δ 161.0, 156.6, 150.9, 139.9, 137.4, 136.3, 129.4, 128.7, 126.3, 125.6, 125.0, 114.3, 101.9, 61.9, 53.2, 33.2, 25.5, 24.1, 22.8, 21.1, 13.21. HRMS (ESI) calcd for $C_{26}H_{34}N_5O_3$ $(M+1)^+$464.2662; found 464.2659.

Compound 21. Column chromatography with (DCM/MeOH: 97/3) gave compound **21** as a solid (212 mg, 85%). M.p. 106-108 °C. ^{1}H NMR (400 MHz, MeOD): δ 8.32 (bs, 2H), 7.31 (*AB* system, *J* = 8.0 Hz, 4 H), 6.85 (s, 1 H), 6.32 (s, 1H), 3.66 (s, 2 H), 3.39 (q, *J* = 7.2 Hz, 2 H), 3.13-3.06 (m, 1 H), 2.58-2.54 (m, 4 H), 1.81-1.77 (m, 4 H), 1.21 (t, *J* = 7.2 Hz, 3 H), 1.06 (d, *J* = 6.8 Hz, 6 H). ^{13}C NMR (100 MHz, MeOD): δ 161.0, 156.6, 150.9, 140.0, 138.2, 137.4, 129.5, 128.0, 126.2, 125.2, 125.0, 114.4, 101.9, 59.0, 53.4, 33.2, 25.5, 22.1, 21.1, 13.1. HRMS (ESI) calcd for $C_{25}H_{32}N_5O_3$ $(M+1)^+$ 450.2505; found 450.2503.

Compound 22. Column chromatography on silica gel previously conditioned with ammonia (DCM/MeOH: 95/5 to 90/10) gave compound **22** as a white solid. M.p. 110-112 °C (132 mg, 54%). ^{1}H NMR (400 MHz, MeOD): δ8.26 (bs, 2H), 7.71 (s, 1 H), 7.25 (*AX* system, *J* = 8.0 Hz, 4 H), 7.06 (s, 1 H), 6.96 (s, 1 H), 6.88 (s, 1 H), 6.32 (s, 1 H), 5.17 (s, 2 H), 3.37 (q, *J* =7.2 Hz, 2 H), 3.14-3.05 (m, 1 H), 1.20 (t, *J* = 7.2 Hz, 3 H), 1.06 (d, *J* = 6.8 Hz, 6 H). ^{13}C NMR (100 MHz, MeOD): δ 161.0, 156.6, 150.6, 139.7, 137.5, 136.7, 129.9, 127.3, 126.4, 126.1, 125.9, 125.0, 119.2, 114.3, 101.9, 49.4, 33.2, 25.5, 21.1, 13.2. HRMS (ESI) calcd for $C_{24}H_{27}N_6O_3$ $(M+1)^+$447.2145; found 447.2143.

Compound 23. Column chromatography (DCM/MeOH: 88/12). The title compound was obtained as a purple oil (162 mg, 58%). ^{1}H NMR (400 MHz, MeOD): δ 7.36 (s, 5 H), 6.85 (s, 1 H), 6.33 (s, 1 H), 4.83 (bs, 4 H), 4.17 (d, *J* = 13.2 Hz, 1 H), 3.72-3.59 (m, 2 H), 3.56 (, *J* = 13.2 Hz, 1 H), 3.39 (q, *J* = 7.2 Hz, 2 H), 3.10 (qn, *J* = 6.8 Hz, 1 H), 2.87-2.84 (m, 1 H), 2.76-2.72 (m, 1 H), 2.35-2.31 (m,1 H), 2.08-2.03 (m, 1 H), 1.82-1.35 (m, 6 H), 1.20 (t, *J* = 7.2 Hz, 3 H), 1.03 (d, *J* = 6.8 Hz, 6 H). ^{13}C NMR (100 MHz, MeOD): δ 160.9, 150.2, 149.9, 144.0, 138.1, 130.2, 130.0, 127.7, 127.4, 126.1, 122.0, 119.8, 105.7, 61.6, 60.2, 58.5, 52.0, 34.3, 33.3, 28.4, 25.4, 25.3, 22.8, 22.7, 14.7.HRMS (ESI) calcd for $C_{28}H_{38}N_5O_4$ $(M+1)^+$508.2924; found 508.2921.

Compound 24. Column chromatography (DCM/MeOH: 90/10) gave compound **24** as a reddish oil (136 mg, 55%). ^{1}H NMR (400 MHz, MeOD): δ 7.33 (*AB* system, *J* = 8.4 Hz, 4 H), 6.84 (s, 1 H), 6.32 (s, 1 H), 4.83 (bs, 3 H), 3.73 (s, 2 H), 3.39 (q, *J*= 7.2 Hz, 2 H), 3.10 (qn, *J* = 6.8 Hz, 1 H), 2.65

(q, J = 7.2 Hz, 4 H), 1.21 (t, J = 7.2 Hz, 3 H), 1.11-1.06 (m, 12 H). ^{13}C NMR (100 MHz, MeOD): δ 160.9, 150.2, 149.9, 144.0, 143.3, 130.0, 128.6, 128.1, 127.0, 126.0, 122.0, 119.8, 105.7, 61.2, 46.7, 34.3, 25.3, 22.7, 14.7, 11.8. HRMS (ESI) calcd for $C_{25}H_{34}N_5O_3$ $(M+1)^+$ 452.2662; found 452.2664.

Compound 25. Column chromatography (DCM/MeOH: 90/10) gave compound **25** as a purple oil (185 mg, 72%). ^{1}H NMR (400 MHz, MeOD): δ 7.30 (s, 5 H), 6.85 (s, 1 H), 6.33 (s, 1 H), 4.88 (bs, 4 H), 3.63 (s, 2 H), 3.60 (t, J = 6.2 Hz, 2 H), 3.39 (q, J = 7.2 Hz, 2 H), 3.11 (qn, J = 6.8 Hz, 1 H), 2.61 (t, J = 6.2 Hz, 2 H), 2.54 (q, J = 7.2 Hz, 2 H), 1.21 (t, J = 7.2 Hz, 2 H), 1.07 (d, J = 6.8 Hz, 6 H), 1.02 (t, J = 7.2 Hz, 3 H). ^{13}C NMR (100 MHz, MeOD): δ 161.1, 156.5, 150.87, 140.1, 139.6, 137.4, 129.3, 127.8, 126.3, 125.0, 124.7, 114.4, 101.9, 58.6, 57.2, 54.2, 47.0, 33.2, 25.5, 21.1, 13.2, 9.9. HRMS (ESI) calcd for $C_{25}H_{34}N_5O_4$ $(M+1)^+$ 468.2611; found 468.2608

Compound 26. Column chromatography (DCM/MeOH: 75/25) gave compound **26** a white solid (102 mg 40%). M.p. 79-81 °C. ^{1}H NMR (400 MHz, MeOD): δ 8.16 (bs, 2H), 7.30 (*AB* system, J = 8.0 Hz, 4 H), 6.84 (s, 1 H), 6.35 (s, 1 H), 3.53 (s, 2 H), 3.39 (q, J = 7.2 Hz, 2 H), 3.17-3.07 (m, 1 H), 3.04 (t, J = 4.8 Hz, 4 H), 2.55 (m,6H), 1.21 (t, J = 7.2 Hz, 3 H), 1.06 (d, J = 6.8 Hz, 6 H). ^{13}C NMR (100 MHz, MeOD): δ 161.0, 156.6, 150.9, 140.0, 137.9, 137.4, 129.4, 127.9, 126.2, 125.1, 124.9, 114.4, 101.9, 61.4, 50.3, 43.4, 33.2, 25.5, 21.1, 13.1. HRMS (ESI) calcd for $C_{25}H_{33}N_6O_3$ $(M+1)^+$465.2614; found 465.2610.

Compound 27. Column chromatography (DCM/MeOH: 88/12) gave compound **27** a pale yellow solid (121 mg, 46%). ^{1}H NMR (400 MHz, MeOD): δ 8.10 (βσ, 2H), 7.29 (*AB* system, J = 8.0 Hz, 4 H), 6.84 (s, 1 H), 6.33 (s, 1 H); 3.50 (s, 2 H), 3.39 (q, J = 7.2 Hz, 2 H), 3.14-3.07 (m, 1 H), 2.60-2.40 (m, 9 H), 2.32 (s, 3 H), 1.21 (t, J = 7.2 Hz, 3 H), 1.06 (d, J = 6.4 Hz, 6 H). ^{13}C NMR (100 MHz, MeOD): δ 161.0, 156.5, 150.8, 140.0, 138.0, 137.4, 129.4, 128.0, 126.3, 125.1, 124.9, 114.4, 101.91, 61.4, 53.6, 51.3, 43.8, 33.2, 25.5, 21.1, 13.2. HRMS (ESI) calcd for $C_{26}H_{35}N_6O_3$ $(M+1)^+$ 479.2771; found 479.2767.

Compound 28. Column chromatography (DCM/MeOH: 93/7) gave compound **28** as a purple oil (58%). ^{1}H NMR (400 MHz, $CDCl_3$): δ 7.37-7.15 (m, 6 H), 7.09 (s, 1 H), 6.41 (s, 1 H), 4.94 (s, 2 H), 4.75 (s, 2 H), 3.89 (s, 3 H), 3.28-3.21 (bm, 2H), 2.88 (d, *J* = 11.2 Hz, 2 H), 2.29 (s, 6 H), 2.22-2.16 (m, 1 H), 1.95 (t, *J* = 11.2 Hz, 2 H), 1.78 (d, *J* = 12.0 Hz, 2 H), 1.57-1.48 (m, 2 H), 1.11 (d, *J* = 6.8 Hz, 6 H). ^{13}C NMR (100 MHz, $CDCl_3$): δ 161.3, 157.3, 151.3, 142.4, 139.8, 135.9, 135.64, 134.9, 130.0, 129.3, 128.2, 128.1, 127.9, 127.6, 127.5, 126.6, 126.4, 125.6, 124.0, 117.3, 98.5, 70.4, 69.9, 62.1, 61.9, 52.6, 51.5, 41.0, 27.6, 25.9, 22.1. HRMS (ESI) calcd for $C_{28}H_{39}N_6O_3$ $(M+1)^+$507.3084; found 507.3080.

Compound 29. Column chromatography on silica gel previously conditioned with ammonia (DCM/MeOH:85/15 to 60/40) gave compound **29** as a waxy material that solidified on standing (113 mg, 42%). ^{1}H NMR (400 MHz, MeOD): δ 8.94 (bs, 2H), 7.29 (*AB* system, *J* = 8.0 Hz, 4H), 6.84 (s, 1 H), 6.33 (s, 1 H), 3.59 (q, *J* = 7.2 Hz, 2 H), 3.39 (q, *J* = 7.2 Hz, 2 H), 3.13-3.07 (m, 1 H), 2.94-2.78 (m, 2 H), 2.71-2.65 (m, 1 H), 2.56-2.50 (m, 1 H), 2.36-2.32 (m, 1 H), 2.26 (s, 6 H), 2.09-1.97 (m, 1 H), 1.78-1.67 (m, 1 H), 1.21 (t, *J* = 7.2 Hz, 3 H), 1.07 (d, *J* = 6.8 Hz, 6 H). ^{13}C NMR (100 MHz, $CDCl_3$): δ 161.0, 156.5, 150.8, 140.0, 138.8, 129.4, 127.6, 126.3, 125.0, 114.4, 101.9, 64.6, 59.0, 56.0, 52.2, 41.7, 33.2, 27.4, 25.5, 21.1, 13.1. HRMS (ESI) calcd for $C_{27}H_{37}N_6O_3$ $(M+1)^+$ 493.2923; found 493.2919.

Compound 30. Column chromatography (DCM/MeOH: 95/5) gave compound **30** as a purple oil (79 mg, 30%). ^{1}H NMR (400 MHz, MeOD): δ 7.98 (bs, 2H), 7.39 (*AB* system, *J* = 8.4 Hz, 4 H), 6.91 (s, 1 H), 6.30 (s, 1 H), 4.01 (s, 2 H), 3.39 (q, *J* = 7.2 Hz, 2 H), 3.14-3.05 (m, 1 H), 2.88-2.80 (m, 1 H), 2.08-2.03 (m, 3 H), 1.85-1.80 (m, 3 H), 1.68 (d, *J* = 12.0 Hz, 1 H), 1.35-1.26 (m, 5 H), 1.21 (t, *J* = 7.2 Hz, 3 H), 1.09 (d, *J* = 6.8 Hz, 6 H). ^{13}C NMR (100 MHz, MeOD): δ 160.9, 156.7, 150.9, 139.8, 137.6, 135.1, 130.0, 127.9, 126,4, 126.2, 125.1, 114.3, 101.8, 56.2, 33.2, 29.69, 25.6, 24.6, 23.9, 21.1, 13.1. HRMS (ESI) calcd for $C_{27}H_{36}N_5O_3$ $(M+1)^+$ 478.2818; found 478.2821.

Compound 31. Column chromatography (DCM/MeOH: 90/10) gave compound **31** as a white solid (113 mg, 42%). M.p. 77-79 °C. ^{1}H NMR (400 MHz, MeOD): δ8.25 (bs, 2 H), 7.35 (*AB* system, *J* = 8.4 Hz, 4 H), 6.88 (s, 1 H), 6.31 (s, 1 H), 3.86 (s, 2 H), 3.39 (q, *J* = 7.2 Hz, 2 H), 3.15-3.05 (m, 1 H), 2.52 (d, *J* = 6.8 Hz, 2 H), 1.78-1.50 (m, 8H), 1.27-1.24 (m, 3 H), 1.21 (t, *J* = 7.2 Hz, 3 H), 1.08 (d, *J* = 6.8 Hz, 6 H), 0.99-0.87 (m, 2 H). ^{13}C NMR (100 MHz, MeOD): δ 161.0, 156.6, 150.9, 139.9, 137.5, 137.1, 129.7, 127.6, 126.2, 125.7, 125.4, 114.3, 101.9, 54.0, 51.6, 35.9, 33.2, 30.2, 25.5, 25.0, 21.1, 13.1. HRMS (ESI) calcd for $C_{28}H_{38}N_5O_3$ $(M+1)^+$ 492.2975; found 492.2977.

Compound 32. Column chromatography (DCM/MeOH: 80/20) gave compound **32** as a white solid (120 mg, 43%). M.p. < 50 °C. ^{1}H NMR (400 MHz, MeOD): δ 7.86 (bs, 2 H), 7.33 (*AB* system, *J* = 8.0 Hz, 4 H), 6.89 (s, 1 H), 6.31 (s, 1 H), 3.84 (s, 2 H), 3.65 (t, *J* = 4.4 Hz, 4 H), 3.39 (q, *J* = 7.2 Hz, 2 H), 3.14-3.07 (m, 2 H), 2.72 (m, 3 H), 2.48 (t, *J* = 6.4 Hz, 2 H), 2.38 (t, *J* = 4.4 Hz, 4 H), 1.21 (t, *J* = 7.2 Hz, 3 H), 1.08 (d, *J* = 6.8 Hz, 6 H). ^{13}C NMR (100 MHz, MeOD): δ 161.0, 156.6, 150.8, 140.0, 138.4, 137.6, 129.7, 127.3, 126.3, 125.4, 125.0, 114.3, 101.8, 65.9, 55.9, 52.8, 51.5, 43.4, 33.2, 25.5, 21.1, 13.1. HRMS (ESI) calcd for $C_{27}H_{37}N_6O_4$ $(M+1)^+$ 509.2876; found 509.2876.

Compound 33. Column chromatography on silica gel previously conditioned with ammonia (DCM/MeOH: 90/10 to 80/20) gave compound **33** as a white solid (87 mg, 32%). M.p. 69-71 °C. ^{1}H NMR (400 MHz, MeOD): δ 8.1 (bs, 2 H), 7.3 (*AB* system, *J* = 8.0 Hz, 4 H), 6.8 (s, 1 H), 6.2 (s, 1 H), 3.7 (s, 2 H), 3.3 (q, *J* = 2 H), 3.1-3.0 (m, 1 H), 2.6-2.5 (m, 6 H), 2.5 (q, *J* = 7.2 Hz, 4 H), 1.2 (t, *J* = 7.2 Hz, 3 H), 1.0 (d, *J* = 7.2 Hz, 6 H), 1.0 (t, *J* = 7.2 Hz, 6 H). ^{13}C NMR (100 MHz, MeOD): δ 161.1, 156.7, 142.0, 140.0, 137.5, 129.5, 127.0, 125.7, 124.9, 114.5, 102.2, 52.2, 50.9, 46.2, 44.8, 33.2, 25.5, 21.2, 13.1, 9.6. HRMS (ESI) calcd for $C_{27}H_{39}N_6O_3$ $(M+1)^+$ 495.3084; found 495.3086.

Compound 34. Column chromatography on silica gel previously conditioned with ammonia (DCM/MeOH 90:10 to 80:20) gave compound **34** as a white solid (89 mg, 35%). M.p. 56-58 °C. ^{1}H NMR (400 MHz, MeOD): δ 7.95 (bs, 2 H), 7.31 (*AB* system, *J* = 8.0 Hz, 4 H), 6.74 (s, 1 H), 6.25 (s, 1 H), 3.71 (s, 2 H), 3.38 (q, *J* = 7.2 Hz, 2 H), 3.11-3.04 (m, 1 H), 2.57-2.45 (m, 10 H), 1.69-

1.62 (m, 2 H), 1.21 (t, J = 7.2 Hz, 3 H), 1.06-1.00 (m, 12 H). ^{13}C NMR (100 MHz, MeOD): δ 161.2, 156.8, 140.0, 139.9, 129.6, 127.0, 124.8, 124.7, 114.8, 102.9, 52.7, 52.2, 50.1, 45.8, 33.2, 25.4, 24.8, 21.2, 13.1, 9.4. HRMS (ESI) calcd for $C_{28}H_{41}N_6O_3$ $(M+1)^+$ 509.3240; found 509.3238.

Compound 35. Column chromatography on silica gel previously conditioned with ammonia (DCM/MeOH 50/50) gave compound **35** as a white solid (95 mg, 35%). M.p. 67-69 °C. ^{1}H NMR (400 MHz, MeOD): δ 8.08 (bs, 2 H), 7.31 (*AB* system, J = 8.4 Hz, 4 H), 6.87 (s, 1 H), 6.30 (s, 1 H), 3.76 (s, 2 H), 3.39 (q, J = 7.2 Hz, 2 H), 3.16-3.07 (m, 1 H), 2.86-2.83 (m, 2 H), 2.49-2.42 (m, 2 H), 2.25 (s, 3 H), 2.01 (t, J = 11.2 Hz, 2 H), 1.91-1.87 (m, 2 H), 1.48-1.38 (m, 3 H), 1.21 (t, J = 7.2 Hz, 3 H), 1.08 (d, J = 6.8 Hz, 6 H). ^{13}C NMR (100 MHz, MeOD): δ 156.6, 150.8, 140.0, 137.8, 137.63, 129.7, 127.4, 126.3, 125.6, 125.1, 114.3, 101.8, 52.7, 52.1, 48.6, 43.3, 33.2, 28.8, 25.5, 21.1, 13.1. HRMS (ESI) calcd for $C_{27}H_{37}N_6O_3$ $(M+1)^+$493.2927; found 493.2923.

Methyl 1-[2,4-bis(benzyloxy)-cumenyl]-5-[*p*-(morpholin-4-ylmethyl)phenyl]-1*H*-1,2,3-triazole-4-carboxylate (36). Et_3N (230 µL, 1.65 mmol) and MsCl (130 µΛ, 1.65 mmol) were added to a solution of **16** (310 mg, 0.55 mmol) in DCM (7 mL) at 0 °C. The solution was stirred for 30 minutes at 0 °C and for 12 hours at rt. The solvent was removed under reduced pressure and the reaction crude was dissolved in DMF (3-4 mL). Morpholine (143 mg, 1.65 mmol) and Et_3N (230 µl, 1.65 mmol) were added and the reaction was stirred for 12 hours at rt. The mixture was diluted with H_2O and EtOAc, the organic phase was extracted four times with EtOAc (4 x 30 ml) and washed with H_2O (2 x 30 mL) and with brine (2 x 30 ml). The solvent was evaporated. Column chromatography (DCM/MeOH: 98/2) gave the title compound as a pale yellow oil (372 mg, 75%). ^{1}H NMR (400 MHz, CD_3Cl): δ 7.37-7.22 (m, 10 H), 7.17 (d, J = 8.4 Hz, 2 H), 7.08 (s, 1 H), 7.01-6.99 (m, 2 H), 6.40 (s, 1 H), 4.93 (s, 2 H), 4.74 (s, 2 H), 3.88 (s, 3 H), 3.67 (t, J = 4.4 Hz, 4 H), 3.47 (s, 2 H), 3.24 (qn, J = 6.8 Hz, 1 H), 2.42-2.38 (m, 4 H), 1.10 (d, J = 6.8 Hz, 6 H). ^{13}C NMR (100 MHz, CD_3Cl): δ 160.6, 158.4, 156.9, 151.3, 140.0, 139.2, 136.6, 136.0, 131.9, 130.7, 128.4, 128.4,

128.4, 128.0, 127.8, 127.8, 127.6, 126.6, 125.2, 121.1, 100.2, 70.3, 70.1, 67.1, 63.2, 53.8, 52.0, 26.3, 22.8.

(2-Chloroethylamino)(1-(2,4-dihydroxycumenyl)-5-[*p*-(morpholin-4-ylmethyl)phenyl]-1*H*-1,2,3-triazol-4-yl)formaldehyde(37) General procedure. Compound **36** (50 mg, 0.07 mmol) was dissolved in a mixture of THF/H_2O (2 mL) containing LiOH (5 mg, 0.2 mmol) and stirred at rt for 12 h. The solvent was evaporated under vacuum and the crude product treated directly with oxalyl chloride (1 mL). The vial was stirred for 2 h and the oxalyl chloride evaporated under vacuum. The residue was dissolved in dry DCM (2 mL) cooled to 0°C and DIPEA (0.2 mL, 2 mmol) and 2-chloroethylamine hydrochloride (58 mg, 0.5 mmol) were subsequently added. The mixture was stirred at rt for 12 h, then the solvent evaporated and the residue treated with EtOAc and passed through a short cartridge containing silica gel (eluting with EtOAc). The collected elute was dried on anhydrous $MgSO_4$, the solvent evaporated and treated several times with dry toluene that was further evaporated in order to remove azeotropically any trace of water. The residue was dissolved in DCM (0.1 mL), cooled to 0 °C and treated with 0.2 mL of a 1 M solution of BCl_3 in DCM. After stirring for 2 h at rt, the solvent was evaporated and the residue purified by column chromatography (DCM:MeOH: 96/4) to give compound **37** as a waxy material (11 mg, 31 % yield). ^{1}H NMR (300 MHz, DMSO-d6) δ: 9.70 (bs, 2H), 8.75 (t, *J* = 5.8 Hz, 1H), 7.25 (d, *J* = 8.4 Hz, 2H), 7.20 (d, *J* = 8.4 Hz, 2H), 6.90 (s, 1H), 6.37 (s, 1H), 3.70 (t, *J* = 6.0, *J* = 6.7 Hz, 2H), 3.51-3.57 (m, 6H), 3.4 (bs, 2H), 3.00 (hept., *J* = 6.9 Hz, 1H), 2.27-2.30 (m, 4H), 0.99 (d, *J* = 6.9 Hz, 6H). ^{13}C NMR (75 MHz, DMSO-d6) δ: 160.7, 150.2, 149.9, 142.0, 140.3, 130.3, 130.0, 128.4, 127.8, 127.7, 122.0, 120.6, 105.7, 67.1, 63.2, 53.8, 43.7, 41.9, 25.3, 22.7. HRMS (ESI) calcd for $C_{25}H_{31}ClN_5O_4$ $(M+1)^+$ 502.2035 (32.4 %), 500.2065 (100 %); found 502.2034 (32 %), 500.2061 (100 %).

Compound 38. Column chromatography (DCM/MeOH: 98/2) gave compound **38** as a waxy material (15 mg, 42%). ^{1}H NMR (300 MHz, DMSO-d6) δ: 9.78 (bs, 1H), 9.70 (bs, 1H), 8.49 (t, *J* = 5.9Hz, 1H), 7.23 (d, *J* = 8.5 Hz, 2H), 7.19 (d, *J* = 8.5 Hz, 2H), 6.87 (s, 1H),6.37 (s, 1H), 3.51-3.54 (m, 4H), 3.39 (s, 2H), 3.16-3.22 (m, 2H), 3.00 (hept., *J* = 6.7 Hz, 1H), 2.29-2.30 (m, 4H), 1.45-1.48

(m, 2H), 1.22-1.25 (m, 7H), 1.01 (d, *J* = 6.9 Hz, 6H), 0.84 (t, *J* = 6.6 Hz, 3H). ^{13}C NMR (75 MHz, DMSO-d6) δ: 160.7, 150.2, 149.9, 143.9, 140.3, 130.4, 130.0, 128.4, 127.7, 127.7, 122.0, 120.6, 105.7, 67.1, 63.2, 53.8, 40.7, 31.7, 27.6, 26.0, 25.3, 22.8, 22.7, 14.1.HRMS (ESI) calcd for $C_{30}H_{41}N_5O_4Na$ $(M+Na)^+$559.3090 (32.4 %), 558.30565 (100 %); found 559.3087 (33 %), 558.30567 (100 %).

Compound 39. Column chromatography (DCM/MeOH: 96/4) gave compound **39** as waxy material (13 mg, 38%). ^{1}H NMR (300 MHz, DMSO-d6) δ: 9.69 (s, 1H),9.66 (s, 1H), 8.28 (d, *J* = 7.8 Hz, 1H), 7.23 (d, *J* = 8.5 Hz, 2H), 7.20 (d, *J* = 8.5 Hz, 2H), 6.87 (s, 1H), 6.37 (s, 1H),4.10-4.22 (m, 1H), 3.52-3.55 (m, 4H),3.41 (bs, 2H), 3.00 (hept., *J* = 6.9 Hz, 1H),2.30 (bs, 4H),1.45-1.90 (m, 8H),0.99 (d, *J* = 6.9 Hz, 6H). ^{13}C NMR (75 MHz, DMSO-d6) δ 160.8, 150.2, 149.9, 144.6, 140.3, 130.4, 130.0, 128.4, 127.8, 127.7, 122.1, 120.6, 105.7, 67.1, 63.2, 53.8, 50.2, 32.6, 25.3, 23.1, 22.7. HRMS (ESI) calcd for $C_{28}H_{35}N_5O_4Na$ $(M+Na)^+$ 529.2620 (30.3 %), 528.2587 (100 %); found 529.2623 (31%), 528.2590 (100 %).

Compound 40. Column chromatography (DCM/MeOH: 98/2) gave compound **40** as waxy material (15 mg, 42%). ^{1}H NMR (300 MHz, DMSO-d6) δ 9.74 (bs, 1H), 9.69 (bs, 1H), 8.19 (d, *J* = 8.6 Hz, 1H), 7.23 (d, *J* = 8.4 Hz, 2H), 7.19 (d, *J* = 8.4 Hz, 2H), 6.87 (s, 1H), 6.37 (s, 1H), 3.69 (bs, 1H), 3.51-3.54 (m, 4H), 3.39 (bs, 2H), 3.00 (hept., *J* = 6.7 Hz, 1H), 2.28-2.30 (m, 4H), 1.54-1.75 (m, 5H), 1.18-1.41 (m, 5H), 0.99 (d, *J* = 6.7 Hz, 6H). ^{13}C NMR (75 MHz, DMSO-d6) δ160.8, 150.2, 149.9, 144.6, 140.3, 130.4, 130.0, 128.4, 127.8, 127.7, 122.1, 120.6, 105.7, 67.1, 63.2, 53.8, 48.1, 32.4, 25.4, 25.3, 25.2, 22.7. HRMS (ESI) calcd for $C_{29}H_{38}N_5O_4$ $(M+1)^+$ 520.2924: found 520.2927.

Compound 41. Column chromatography (DCM/MeOH: 95/5) gave compound **41** as waxy material (8 mg, 22%). ^{1}H NMR (300 MHz, DMSO-d6) δ 9.76 (bs, 2H), 7.26 (d, *J* = 8.1 Hz, 2H), 7.17 (d, *J* = 8.1 Hz, 2H), 6.99 (s, 1H), 6.40 (s, 1H), 3.51-3.54 (m, 8H), 3.41 (bs, 2H), 3.2-3.3 (bm, 4H), 3.04 (hept., *J* = 6.9 Hz, 1H), 2.27-2.30 (m, 4H), 1.03 (d, *J* = 6.9 Hz, 6H). ^{13}C NMR (75 MHz, DMSO-

d6) δ: 162.6, 150.2, 149.9, 143.5, 140.3, 130.3, 130.0, 128.4, 127.8, 127.7, 122.0, 120.6, 105.7, 67.1, 66.4, 63.2, 53.8, 45.3, 44.6, 25.3, 22.8. HRMS (ESI) calcd for $C_{27}H_{34}N_5O_5$ $(M+1)^+$ 508.2560; found 508.2563.

Compound 42.The desired amide was obtained after purification by preparative HPLC using a gradient of a binary mixture of H_2O/CH_3CN further containing 0.1% TFA from 90/10 to 10/90. Obtained 7 mg of **42** (19 %). ^{1}H NMR (300 MHz, MeOD):δ 7.44-7.51 (m, 4H), 7.46 (d, *J* = 8.7 Hz, 2H), 6.97 (s, 1H), 6.31 (s, 1H), 4.49 (m, 1H), 4.33 (bs, 2H), 3.88 (bs, 4H) 3.27 (bs, 4H), 3.12 (hept., *J* = 6.9 Hz, 1H), 2.31 (m, 1H), 1.10 (d, *J* = 6.9 Hz, 6H), 1.04 (d, *J* = 6.9 Hz, 6H). ^{13}C NMR (75 MHz, DMSO-d6) δ 174.5, 158.9, 150.2, 149.9, 142.9, 140.3, 130.3, 130.0, 128.4, 127.8, 127.7, 122.0, 120.6, 105.7, 67.1, 63.2, 58.6, 53.8, 31.2, 25.3, 22.8, 19.3, 18.2. HRMS (ESI) calcd for $C_{28}H_{35}N_5O_6$ M^+ 537.2588; found 537.2586.

Compound 45. Methyl 7-aminoheptanoate HCl (31 mg, 0.16 mmol), DIPEA (51 μL, 0.28 mmol) and PyBOP (62 mg, 0.12 mmol) were added to a solution of acid obtained from **36** as previously described(62 mg, 0.10 mmol) in 4 mL of DCM. The reaction mixture was stirred at rt until complete conversion (6h, TLC check with eluent DCM/MeOH:96/4) then diluted with DCM and washed with H_2O. The organic phase was dried over Na_2SO_4 and concentrated at reduced pressure. The crude product was purified by flash chromatography (DCM/MeOH: 98/2) to give **45** (46 mg, 58%). ^{1}H-NMR (300 MHz, DMSO-d6) δ: 8.57 (t, 1H, J = 5.7 Hz), 7.43 (m, 5H), 7.31 (m, 5H), 7.23 (s, 1H), 7.19 (m, 4H), 6.91 (s, 1H), 5.13 (s, 2H), 4.97 (s, 2H), 3.57 (s, 3H), 3.54 (m, 4H), 3.43 (s, 2H), 3.21 (m, 2H), 3.16 (m, 1H), 2.31 (bm, 4H), 2.28 (t, 2H, J = 7.3 Hz), 1.51 (m, 4H), 1.27 (m, 4H). 1.06 (d, 6H, J = 7.1 Hz).^{13}C NMR (75 MHz, MeOD) δ 173.5, 160.7, 158.4, 156.8, 143.9, 140.3, 136.6, 136.0, 131.2, 130.8, 128.4, 128.3, 127.9, 127.8, 127.7, 127.6, 126.6, 124.9, 120.9, 100.4, 70.3, 70.1, 67.1, 63.2, 53.8, 51.1, 40.4, 33.6, 28.8, 27.0, 26.3, 25.4, 25.0, 22.8. ESI-MS m/z = 782.4 $[M+Na]^+$.

Compound 46. BCl_3 1M in DCM (240 μL, 0.24 mmol) was added to a solution of **45** (46 mg, 0.06 mmol) in DCM (2 mL) stirred at 0 °C. The reaction mixture was allowed to warm up to rt and after

3 h the conversion of **45** was complete. Ethyl acetate was added and the mixture was washed with a satured solution of $NaHCO_3$. The aqueous phase was extracted 3 times with EtOAc and organic phases were collected, dried over Na_2SO_4, filtered and concentrated at reduced pressure. The crude product was purified by flash chromatography (DCM/MeOH:95/5) to give the desired product (35 mg, 93%). ^{1}H-NMR (300 MHz, DMSO-d6) δ 9.70(bs, 1H), 9.65 (s, 1H), 8.51 (t, 1H, J = 5.8 Hz), 7.21 (m, 4H), 6.84 (s, 1H), 6.38 (s, 1H), 3.56 (s, 3H), 3.51 (bs, 4H), 3.40 (bs, 2H), 3.20 (m, 2H), 3.02 (m, 1H), 2.25 (m, 6H), 1.47 (m, 4H), 1.28 (m, 4H), 1.05 (d, 6H, J = 7.0 Hz). ESI-MS m/z = 782.4 $[M+Na]^+$, 758.3 $[M-H]^-$.

Compound 43. Hydroxylamine (50% acqueous solution, 50 μL, 0.75 mmol) and 1M NaOH (500 μL, 0.50 mmol) were added to a stirred solution of **46** (30 mg, 0.05 mmol) in MeOH (500 μL, 0.1M) at 0 °C. The reaction mixture was warmed up to rt and, after 2 h, TLC analysis showed complete conversion of starting material. The solution was extracted with AcOEt and the organic phase was washed with water and brine, dried over Na_2SO_4 and concentrated under reduced pressure. The crude product was purified by preparative HPLC with TFA buffered eluents to give salified **43** (18 mg, 49%). ^{1}H-NMR (300 MHz, DMSO-d6): δ 10.35 (bs, 2H), 9.75 (bs, 2H), 8.58 (t, J = 5.6 Hz, 1H), 7.40 (m, 4H), 6.94 (s, 1H), 6.39 (s, 1H), 4.30 (s, 2H), 3.92 (bm, 2H), 3.65 (bm, 2H), 3.17 (m, 2H), 3.10 (bm, 4H), 3.01 (m, 1H), 1.90 (t, J = 7.3 Hz, 2H), 1.43 (m, 4H), 1.24 (m, 4H). 1.09 (d, J = 6.9 Hz, 6H). ^{13}C NMR (75 MHz, DMSO-d6): δ 172.4, 160.7, 150.2, 149.9, 143.9, 140.3, 130.4, 130.0, 128.4, 127.8, 127.7, 122.1, 120.6, 105.7, 67.1, 63.3, 53.8, 40.4, 32.1, 27.2, 25.5, 25.4, 25.3, 24.5, 22.8. ESI-MS m/z = 581.3 $[M+H]^+$ESI-MS *m/z* = 579.4 $[M-H]^-$HRMS (ESI) calcd for $C_{30}H_{41}N_6O_6$ $(M+1)^+$ 581.3088; found 581.3085.

Compound 44. Compound **18** (46 mg, 0.1 mmol) was dissolved in acetic anhydride (1 mL) with a catalytic amount of perchlorate (0.2 mmol) and the mixture stirred at rt for 12 h. The acetic anhydride solution was treated with HCl 1 N in order to transform it into acetic acid that was removed by co-distillation with hexane (rotavapor). The solid resulted **44** (48 mg, 92%) was obtained with 100% purity. ^{1}H NMR (400 MHz, MeOD): δ 7.30-7.25 (m, 4 H), 6.82 (s, 1 H), 6.31

(s, 1 H), 4.84 (bs, 3 H), 3.63-3.61 (m, 4 H), 3.46 (s, 2 H), 3.37 (q, J = 7.2 Hz, 2 H), 2.41-2.39 (m, 4 H), 2.08 (s, 6 H), 1.19 (t, J = 7.2 Hz, 3 H), 1.03 (d, J = 6.8 Hz, 6 H). ^{13}C NMR (100 MHz, MeOD) δ 161.0, 156.5, 150.8, 140.0, 137.8, 137.4, 129.4, 128.1, 126.3, 125.1, 125.0, 114.4, 101.8, 65.8, 62.0, 52.7, 33.2, 25.5, 21.1, 20.3, 13.2. HRMS (ESI) calcd for $C_{29}H_{36}N_5O_6$ $(M+1)^+$ 550.2666; found 550.2665.

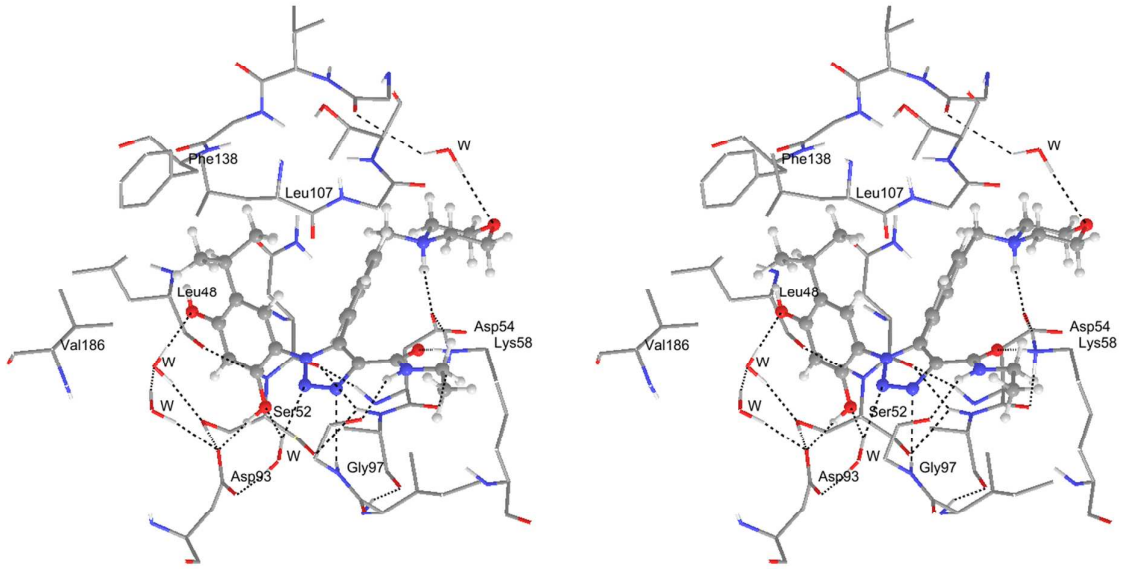

Figure 2: Stereo graphical representation of the complex between Hsp90 and **18** (ball and stick notation) as derived from molecular docking calculations and energy minimization (pdb entry 2VCI, 2.0 Å resolution). The triazole core and the resorcinol hydroxyl groups are involved in an extended network of water-bridged hydrogen bonds. The morpholine solubilizing group is exposed to the solvent and is able to block a water molecule. For the sake of clarity, only few amino acids are displayed and labeled, together with several water molecules (W). Hydrogen bond contacts are depicted as black dotted lines.

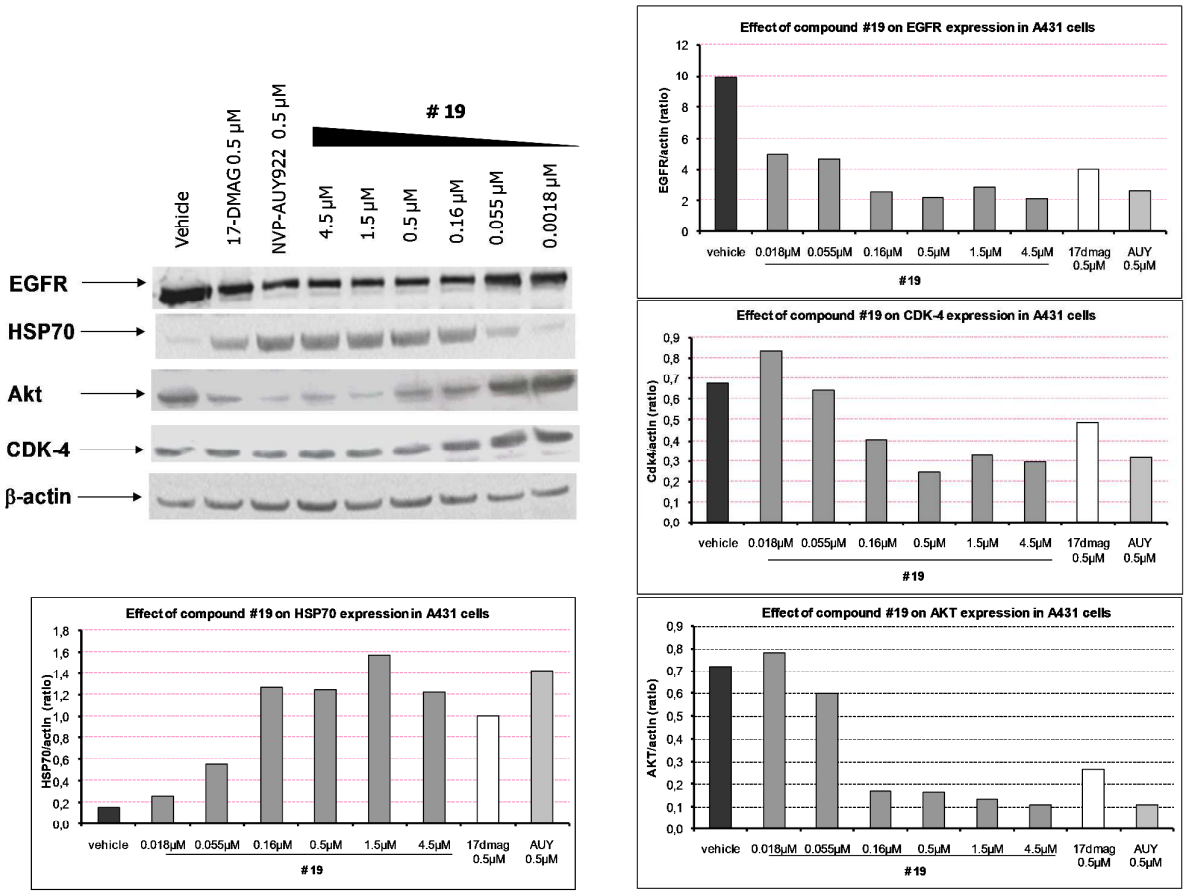

Figure 3: Analysis of Hsp90 client protein levels (EGFR, Akt, CDK-4) and Hsp70 in A431 tumor cells treated with compound **19** *vs.*17-DMAG and NVP-AUY922. Total cellular extracts were obtained 24 h after treatment. Actin is shown as a control for protein loading. A representative blot is shown. Results of densitometry analysis were reported as normalized (to β-actin) ratios. Western blot experiments were performed at least twice resulting in absolutely similar results.

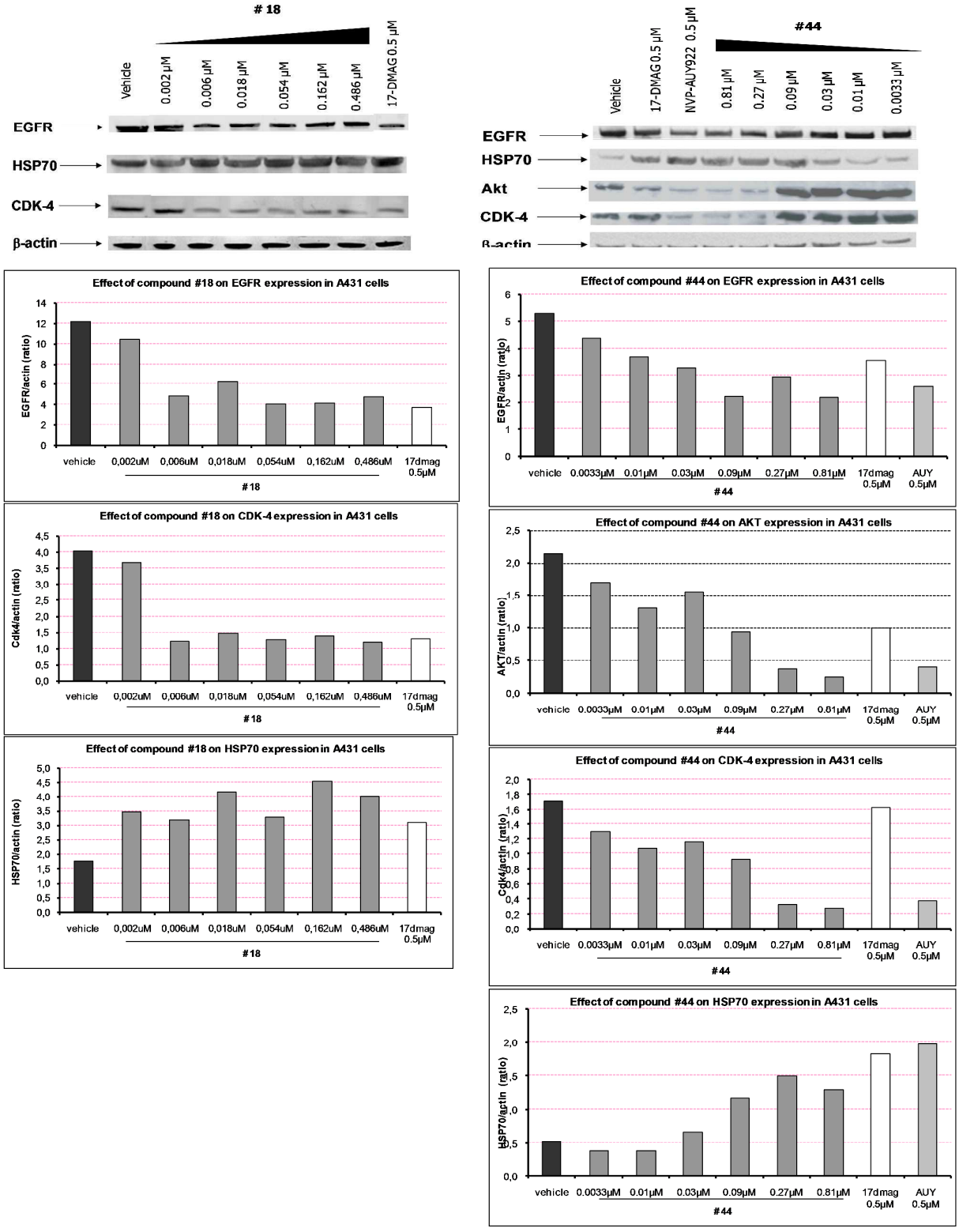

Figure 4: Western Blot analysis of Hsp90 client protein levels in A431 tumor cells treated with the lead compound **18** *vs.* its diacetyl-prodrug (**44**). Analysis was performed as described in Figure 3.

A

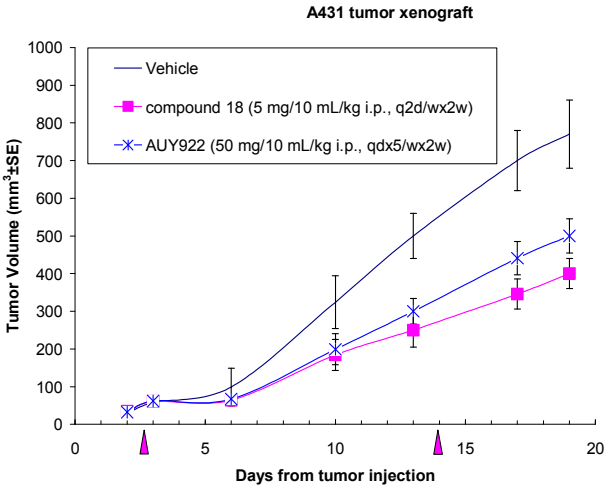
A431 tumor xenograft
Vehicle
compound 18 (5 mg/10 mL/kg i.p., q2d/wx2w)
AUY922 (50 mg/10 mL/kg i.p., qdx5/wx2w)
Tumor Volume (mm3±SE)
Days from tumor injection
0
100
200
300
400
500
600
700
800
900
1000
0
5
10
15
20

B

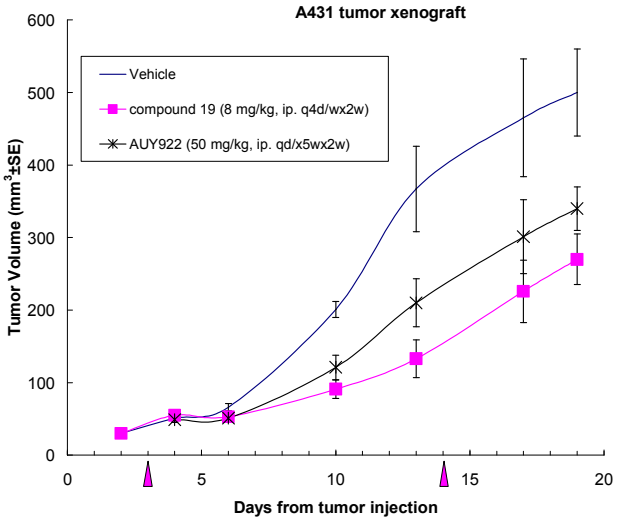
A431 tumor xenograft
Vehicle
compound 19 (8 mg/kg, ip. q4d/wx2w)
AUY922 (50 mg/kg, ip. qd/x5wx2w)
Tumor Volume (mm3±SE)
Days from tumor injection
0
100
200
300
400
500
600
0
5
10
15
20

C

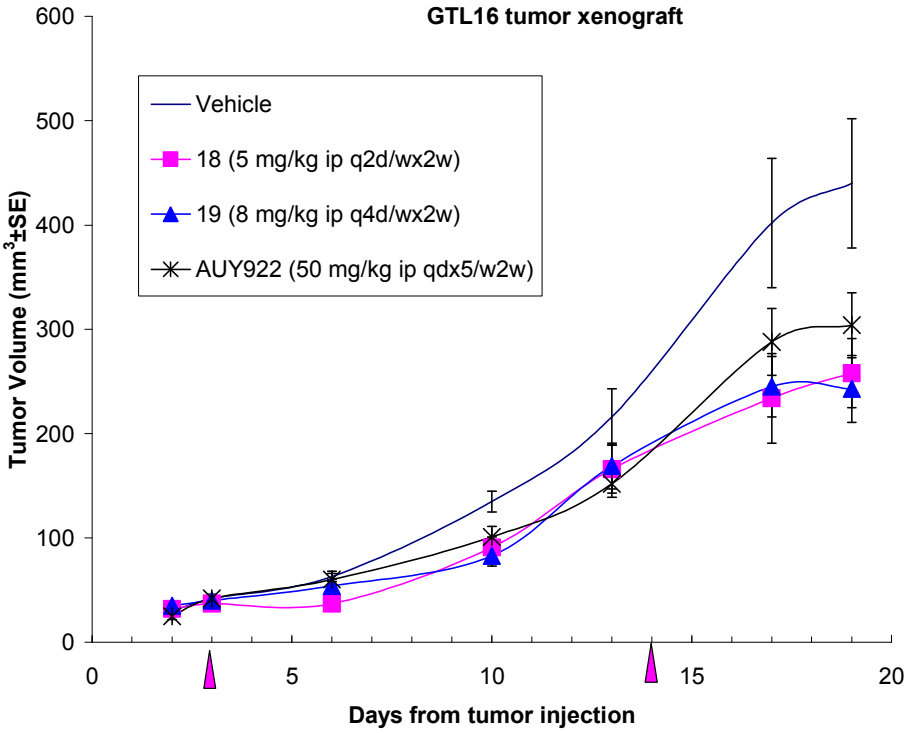

Figure 5: Antitumor efficacy of compounds **18** and **19** delivered intraperitoneally in comparison with NVP-AUY922 against A431 epidermoid carcinoma (overexpressing EGF receptor) (A and B), and GTL-16 gastric carcinoma (overepressing c-Met) (C), xenografted s.c. in nude mice.

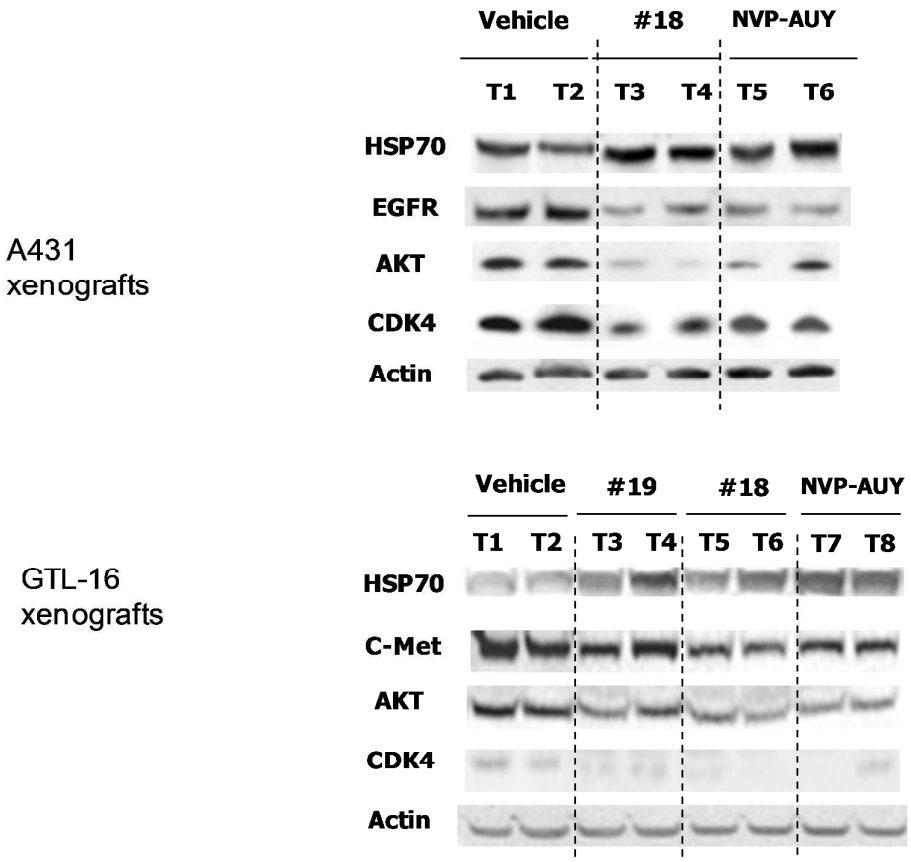

Figure 6: Analysis of Hsp90 client protein levels (EGFR, Akt, CDK-4, c-Met) and Hsp70 in A431 (A) and GTL-16 (B) tumor xenografts, following treatment with **18** and **19**, with respect to the reference compound (NVP-AUY922). Total proteins were purified 2 h (in the case of A431 tumors) or 6 h (in the case of GTL-16 tumors) after the last treatment. Actin is shown as a control for protein loading. Representative blots of two tumor samples/group are shown**.**

Table 1. Data of activity of 1,4- or 1,5-disusbstituted triazoles. Binding on Hsp90 by a fluorescence polarization assay (FP Assay) and cytotoxicity on NCI-H460 non-small cell lung carcinoma cells.

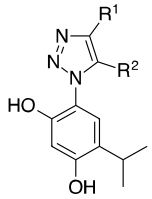

entry	compound	R^1	R^2	Hsp90(FP)[a]	NCI-H460[a]
1	NVP-AUY922	-	-	61±1	2.4±0.06
2	**8**	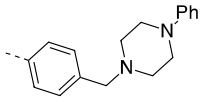	H	320±10	>1000
3	**9**	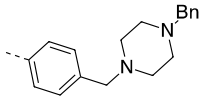	H	295±8	>1000
4	**10**	H	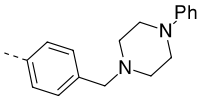	36±1	520±9
5	**11**	H	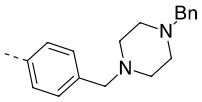	27±1	180±1
6	**12**	H	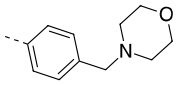	35±1	150±7
7	**13**	H	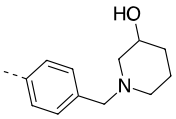	37±1	45±1

a) Binding to Hsp90 determined by a fluorescence polarization assay (FP Assay) and cytotoxicity on NCI-H460 non-small cell lung carcinoma cells. Data are expressed as IC_{50} mean values (± SD, n=4) and are in nanomolar concentrations. For the detection limits of the FP assay see ref. 25.

Table 2. Data of activity for 1,4,5-trisubstituted 1,2,3-triazole carboxamides. Binding on Hsp90 by a fluorescence polarization assay (FP Assay) and cytotoxicity on NCI-H460 non-small cell lung carcinoma cells.

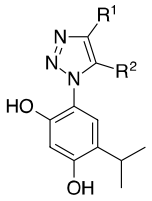

entry	compound	R^1	R^2	Hsp90(FP)[a]	NCI-H460[a]
1	NVP-AUY922	-	-	61±11	2.4±0.06
2	**18**	-$CONHCH_2CH_3$	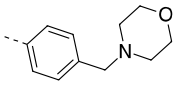	< 5.0	4±0.1
3	**19**	-$CONHCH_2CH_3$	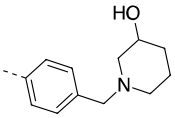	23±1	62±1
4	**(*S*-19)**	-$CONHCH_2CH_3$	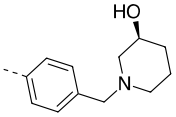	23±1	70±3
5	**(*R*-19)**	-$CONHCH_2CH_3$	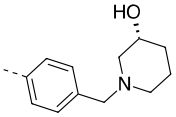	30±1	52±2
6	**20**	-$CONHCH_2CH_3$	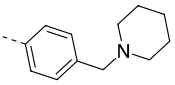	21±1	6±0.2
7	**21**	-$CONHCH_2CH_3$	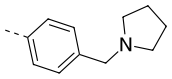	< 5.0	3±0.2
8	**22**	-$CONHCH_2CH_3$	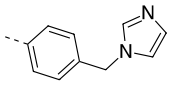	23±1	28±1
9	**23**	-$CONHCH_2CH_3$	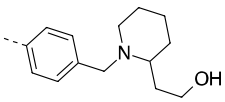	10±1	110±6
10	**24**	-$CONHCH_2CH_3$	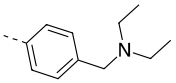	25±1	11±0.7
11	**25**	-$CONHCH_2CH_3$	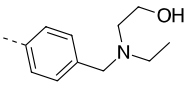	< 5.0	56±2
12	**26**	-$CONHCH_2CH_3$	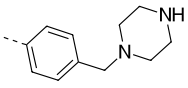	< 5.0	250±11
13	**27**	-$CONHCH_2CH_3$	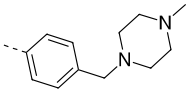	< 5.0	47±2

14	**28**	-CONHCH$_2$CH$_3$	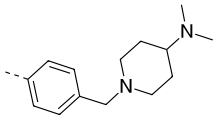	< 5.0	120±6
15	**29**	-CONHCH$_2$CH$_3$	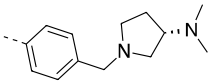	13±1	85±4
16	**30**	-CONHCH$_2$CH$_3$	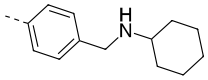	6.8±0.1	15±1
17	**31**	-CONHCH$_2$CH$_3$	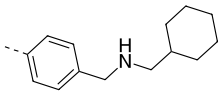	< 5.0	2.1±0.1
18	**32**	-CONHCH$_2$CH$_3$	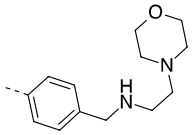	14.8±1	140±6
19	**33**	-CONHCH$_2$CH$_3$	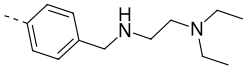	15±1	200±7
20	**34**	-CONHCH$_2$CH$_3$	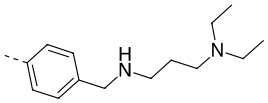	12±1	412±10
21	**35**	-CONHCH$_2$CH$_3$	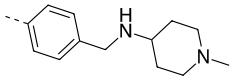	32±1	>1000
22	**37**	-CONH(CH$_2$)$_2$Cl	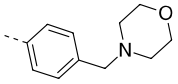	17±1	4.3±0.2
23	**38**	-CONH(CH$_2$)$_6$CH$_3$	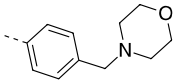	33±1	45±1
24	**39**	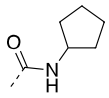	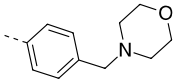	27±1	14±0.7
25	**40**	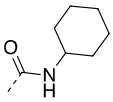	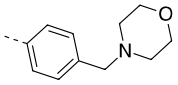	95±3	46±1
26	**41**	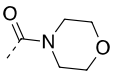	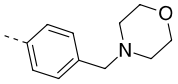	270±3	>1000
27	**42**	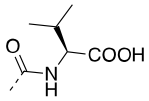	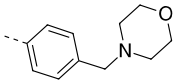	181±5	>1000
28	**43**	- CONH(CH$_2$)$_6$CONHOH	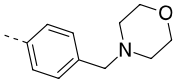	31±1	> 1000
29	**44**	*See Scheme 4*		> 1000	6.5±0.6

[a]: Binding to Hsp90 determined by a fluorescence polarization assay (FP Assay) and cytotoxicity on NCI-H460 non-small cell lung carcinoma cells. Data are expressed as IC_{50} mean values (± SD, n=4) and are in nanomolar concentrations. For the detection limits of the FP assay see ref. 25

Table 3. Antitumor activity of **18** administered i.p. with a schedule (q2d/wx2w), and of **19** given i.p. (q4d/wx2w), on A431 epidermoid carcinoma and GTL-16 (gastric carcinoma) cells implanted subcutaneously on CD-1 nude mice

A431 epidermoid carcinoma.

Compound	[a]Dose (mg/Kg)	[b]BWL (%)	[c]Lethal toxicity	[d]TVI%
18	5	1	0/8	*49
19	8	7	0/8	*45

GTL-16 gastric carcinoma. °

Compound	[a]Dose (mg/Kg)	[b]BWL (%)	[c]Lethal toxicity	[d]TVI%
18	5	17	0/8	*42
19	5	17	0/8	*42

Treatment started 3 days after tumor injection. Efficacy of drugs was evaluated 5 days after the last treatment.

[a] Intraperitoneal dose (mg/10 mL/kg) used in each administration.

[b] Maximum BWL percentage due to the drug treatment.

[c] Dead/treated animals.

[d] TVI percentage versus control mice.

* $P < 0.05$ *vs.* vehicle-treated group (Mann-Whitney test).

°The tumor xenograft induced cachexia.

Table 4. Plasma Stability of Lead compound **18** *vs.* reference compound**.**

Compound	Plasma Stability (%) at 120 min
NVP-AUY922	65.5 ± 1.6
18	56.1 ± 2.2

Data represent the mean ± SD a representative experiment.

Table 5: Different HDAC isoform inhibitory activity (IC50, μM) of **43**, an HDAC/Hsp90 dual inhibitor compared with suberoylamide hydroxamic acid (SAHA)

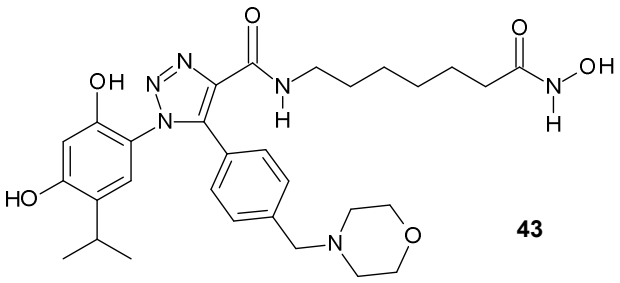

43

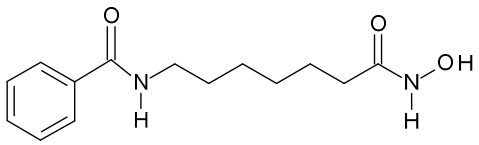

SAHA

HDAC isoforms	1	2	3	4	5	6	7	8	9	10	11
43	3.10	5.61	2.79	71.50	1.91	**0.012**	45.50	0.717	-	3.22	1.77
SAHA (Vorinostat)	0.26	0.92	0.35	0.493	0.378	0.029	0.344	0.243	0.316	0.456	0.362

ASSOCIATED CONTENT

Supporting Information. Synthetic scheme of compound **43**, analysis of Hsp90 client protein levels and the antiproliferative activity of all 1,2,3-triazoles on a panel of tumor cell lines. This material is available free of charge via the Internet at http://pubs.acs.org

AUTHOR INFORMATION

Corresponding Author

For D.S.: phone: +39-0577234275; fax: +39-0577234333; e-mail:maurizio.taddei@unisi.it

For G.G.: phone, +39-0691394441; fax, +39-0691393638; e-mail: giuseppe.giannini@sigma-tau.it

Present Addresses

1) C.P. Biogem S.C.A.R.L., via Camporeale, I-83031 Ariano Irpino (AV) Italy. 2)W.C. Indena, SpA, viale Ortles 12, I-20139 Milano, Italy. 3) M.C. Dipartimento di Chimica "Ugo Schiff", Università degli Studi di Firenze, Via della Lastruccia 3, Sesto Fiorentino (FI) Italy.

Acknowledgment

This work was supported by grants from Sigma-tau Research Switzerland S.A. Sigma-tau Research Switzerland S.A. retains the property rights of all the compounds described in the paper. The authors would like to thank Dr. Tiziana Brunetti and Gianfranco Battistuzzi for their useful support in the preparation of the manuscript.

Abbreviation used

References and notes

1. Sreedhar, A.S.; Csermely, P. Heat shock proteins in the regulation of apoptosis: new strategies in tumor therapy: a comprehensive review. *Pharmacol. Ther.* **2004**, *101*, 227–257.
2. Stravopodis, D.J.;, Margaritis, L. H.; Voutsinas, G.E. Drug-mediated targeted disruption of multiple protein activities through functional inhibition of the Hsp90 chaperone complex. *Curr. Med Chem.* **2007**, *14*, 3122–3138.
3. Banerji, U. Heat shock protein 90 as a drug target: some like it hot. *Clin. Cancer Res.***2009,** *1*, 9–14.
4. Neckers L. Heat shock protein 90: the cancer chaperone. *J Biosci* .**2007**, *32*, 517–530.
5. Ho, N.; Li, A.; Li, S.; Zhang, H. Heat shock protein 90 and role of its chemical inhibitors in treatment of hematologic malignancies. *Pharmaceuticals* **2012**, *5*, 779–801.
6. Taldone, T.; Zatorska, D.; Patel P.D.: Zong H.; Rodina, A: Ahn, J.H.; Moulick, K.; Guzman, M.L.; Chiosis G. Design, synthesis, and evaluation of small molecule Hsp90 probes. *Bioorg. Med. Chem.***2011**, *19*, 2603–2614.
7. Chen, G.; Bradford, W. D.; Seidel, C. W.; Li, R. Hsp90 stress potentiates rapid cellular adaptation through induction of aneuploidy. *Nature,* **2012**, *482*, 246-250.
8. Lu, X.; Wang, L.; Ruden M.D. Hsp90 Inhibitors and the reduction of anti-cancer drug resistance by non-genetic and genetic mechanisms. *Pharmaceuticals,* **2012**, *5*, 890-898.
9. Turbyville,T.J.; Kithsiri Wijeratne, E. M.; Liu, M. X.; Burns, A. M.; Seliga, C. J.; Luevano, L. A.; David, C. L.; Faeth, S.H.; Whitesell, L.; Gunatilaka, A.A.L. Search for Hsp90 inhibitors with potential anticancer activity: isolation and SAR studies of radicicol and monocillin I from two plant-associated fungi of the Sonoran desert. *J. Nat. Prod*. **2006**, *69,* 178–184.

10. Neckers, L.; Workman, P. Hsp90 molecular chaperone inhibitors: are we there yet? *Clin. Cancer Res*. **2012**, *18*, 64–76.

11. Patki, J. M.; Pawar, S. S. Hsp90: chaperone-me-not. *Pathol. Oncol. Res*., **2013**, *19*, 631–640.

12. Chang, D-J.; An, H.; Kim,K-s.; Kim, H.H.; Jung, J.; Lee, M.L.; Kim, N-J.; Han, Y. T.; Yun, H.; Lee, S.; Lee, G.; Lee, S.; Lee, J.S.; Cha, J-H.; Park, J-H.; Park, J. W.; Lee, S-C.; Kim, S.G.; Kim, J. H.; Lee, H.Y.; Kim, K-W.; Suh W-G. Design, synthesis, and biological evaluation of novel deguelin-based heat shock protein 90 (Hsp90) inhibitors targeting proliferation and angiogenesis *J. Med. Chem*. **2012**, *55*, 10863−10884.

13. Soga, S.; Akinaga, S.; Shiotsu, Y. Hsp90 inhibitors as anti-cancer agents, from basic discoveries to clinical development. *Curr. Pharm. Des.* **2013**, *19*, 366-376.

14. Biamonte, M. A.; Van de Water, R.; Arndt, J. W.; Scannevin, R. H.; Perret, D.; Lee, W-C. Heat shock protein 90: inhibitors in clinical trials *J. Med. Chem*. **2010**, *53*, 3–17

15. Richter, K.: Soroka, J.; Skalniak, L.; Leskovar, A.; Hessling, M.; Reinstein, J.; Buchner J, Conserved conformational changes in the ATPase cycle of human Hsp90. *J. Biol. Chem.* **2008**, *283*, 17757–17765

16. Hanessian, S.; Auzzas, L.; Larsson, A.; Zhang, J.; Giannini, G.; Gallo, G.; Ciacci A.; Cabri, W. Vorinostat-like molecules as structural, stereochemical, and pharmacological tools. *ACS Med. Chem. Lett.* **2010**, *1*, 70–74.

17. Botta, C. B.; Cabri, W.; Cini, E.; De Cesare, L.; Fattorusso, C.; Giannini, G.; Persico, M.; Petrella, A.; Rondinelli, F.; Rodriquez, M.; Russo, A.; Taddei, M. Oxime amides as a novel Zinc binding group in histone deacetylase inhibitors: synthesis, biological activity, and computational evaluation. *J. Med. Chem.* **2011**, *54*, 2165–2182.

18. Baruchello, R.; Simoni, D.; Grisolia, G.; Barbato, G.; Marchetti, P.; Rondanin, R.; Mangiola, S.; Giannini, G.; Brunetti, T.; Alloatti, D.; Gallo, G.; Ciacci, A.; Vesci, L.; Castorina, M.; Milazzo, F. M.; Cervoni, M. L.; Guglielmi, M. B.; Barbarino, M.; Foderà,

R.; Pisano, C.; Cabri, W. Novel 3,4-isoxazolediamides as potent inhibitors of chaperone heat shock protein 90. *J. Med. Chem.* **2011**, *54*, 8592–8604.

19. Brough, P. A.; Aherne, W.; Barril, X.; Borgognoni, J.; Boxall, K.; Cansfield, J. E.; Cheung, K-M. J.; Collins, I.; Davies, N. G. M.; Drysdale, M.; J.; Dymock, B.; Eccles, S. E.; Finch, H.; Fink, A.; Hayes, A.; Howes, R.; Hubbard, R. E.; James, K.; Jordan, A. M.; Lockie, A.; Martins, V.; Massey, A.; Matthews, T. P.; McDonald, E.; Northfield, C. J.; Pearl, L. H.; Prodromou, C.; Ray, S.; Raynaud, F. I.; Roughley, S. D.; Sharp, S. Y.; Surgenor, A.; Walmsley, D. L.; Webb, P.; Wood, M.; Workman, P.; Wright L. 4,5-Diarylisoxazole Hsp90 chaperone inhibitors: potential therapeutic agents for the treatment of cancer. *J. Med. Chem.* **2008,** *51,* 196–218.
20. Cikotiene, I.; Kazlauskas, E.; Matuliene, J.; Michailoviene, V.; Torresan, J.; Jachno, J.; Matulis, D. 5-Aryl-4-(5-substituted-2,4-dihydroxyphenyl)-1,2,3-thiadiazoles as inhibitors of Hsp90 chaperone. *Bioorg. Med. Chem. Lett*. **2009**, *19*, 1089-1092.
21. Hong, T-J.: Park H.; Kim Y-J.; Jeong J-H.; Hahn, J-S. Identification of new Hsp90 inhibitors by structure-based virtual screening. *Bioorg. Med. Chem. Lett*. **2009**, *19*, 4839–4842.
22. a) McCleese, J. K.; Bear M. D.; Fossey, S. L.; Mihalek, R. M.; Foley K. P.; Ying, W.; Barsoum, J.; London, C. A. The novel Hsp90 inhibitor STA-1474 exhibits biologic activity against osteosarcoma cell lines. *Int. J. Cancer.* **2009**, *125*, 2792-2801. b) Chimmanamada, D.; Burlinson, J. A.; Ying, W.; Sun, L.; Schweizer, S. M.; Zhang, S.; Demko, Z.; James, D.; Prezwloka, T. Triazole compounds that modulate Hsp90 activity. US2011105483(A1).
23. Majireck, M. M.; Weinreb, S. M. A Study of the scope and regioselectivity of the Ruthenium-catalyzed [3 + 2]-cycloaddition of azides with internal alkynes. *J. Org. Chem.* **2006,** *71,* 8680-8683.
24. Spiteri, C.; Moses J. E. Copper-catalyzed azide–alkyne cycloaddition: regioselective synthesis of 1,4,5-trisubstituted 1,2,3-triazoles. *Angew. Chem. Int. Ed*. **2010**, *49*, 31–33.

25. Due to detection limits of the assay, the most active compounds were reported in Table 2 as having a IC_{50} < 5 nM. However, curve fitting using *Prism GraphPad* software program suggested a binding lower than 3.0 nM for compounds **18**, **21**, **25**, **26**, **27**, while the best IC_{50} value was found for pyrrolidine derivative **21** (IC_{50} = 1 nM). For the limits of the assay see: Kim, J.; Felts, S.; Llauger, L.; He, H.; Huezo, H.; Rosen, N.; Chiosis, G. Development of a fluorescence polarization assay for the molecular chaperone Hsp90. *J. Biomol. Screen.* **2004**, *9*, 375−381.

26. LC/MS analysis showed that compound **44** is stable under conditions employed in the FP assay. For resorcinol esterification in order to get an effective pro-drug see: London, C. A.; Bear, M. D.; McCleese, J.; Foley, K. P.; Paalangara, R.; Inoue, T.; Ying, W.; Barsoum, J. Phase I evaluation of STA-1474, a prodrug of the novel Hsp90 inhibitor ganetespib, in dogs with spontaneous cancer. *PlosOne* **2011**, *6*, e2701.

27. Compound **18** and NVP-AUY922 bind Hsp90 comparably with the diverse STA-9090 (ganatesib): Shimamura, T.; Perera, S.A.; Foley, K.P.; Sang, J.; Rodig, S.J.; Inoue, T.; Chen, L.; Li, D.; Carretero, J.; Li, Y.-C.; Sinha, P.; Carey, C.D.; Borgman, C. L.; Jimenez, J.-P.; Meyerson, M.; Ying, W.; Barsoum, J.; Wong, K.-K.; Shapiro, G.I. Ganetespib (STA-9090), a nongeldanamycin Hsp90 inhibitor, has potent antitumor activity in vitro and in vivo models of non–small cell lung cancer. *Clin. Cancer Res.* **2012**, *18*, 4973-4982.

28. Koga, F.; Tsutsumi, S.; Neckers, LM. Low dose geldanamycin inhibits hepatocyte growth factor and hypoxia-stimulated invasion of cancer cells. *Cell Cycle,* **2007**, *6*, 1393-402.

29. Maulik, G.; Kijima, T.; Ma, PC.; Ghosh, SK.; Lin, J.; Shapiro, G.I.; Schaefer, E.; Tibaldi, E.; Johnson, B.E.; Salgia, R. Modulation of the c-Met/hepatocyte growth factor pathway in small cell lung cancer. *Clin Cancer Res.***2002**, *8*, 620-7.

30. Compounds **18** and **19** were dosed differently and according to different schedules, because the experimental conditions were chosen upon a series of preliminary experiments to identify the best tolerability and efficacy.

31. Screening was performed by Reaction Biology Corp., Malvern, PA. See: Auzzas, L.; Larsson, A.; Matera, R.; Baraldi, A.; Deschênes-Simard, B.; Giannini, G.; Cabri, W.; Battistuzzi, G.; Gallo, G.; Ciacci, A.; Vesci, L.; Pisano, C.; Hanessian, S. Non-natural macrocyclic inhibitors of histone deacetylases: design, synthesis, and activity *J. Med. Chem.*, **2010**, *53*, 8387–8399.

32. a) Kekatpure, V. D.; Dannenberg,A. J.; Subbaramaiah, K. HDAC6 modulates Hsp90 chaperone activity and regulates activation of aryl hydrocarbon receptor signaling. *J. Biol Chem*. **2009**, *284***,** 7436-7445. b) Bali P.; Pranpar, M.; Bradner, J.; Balasis, M.; Fiskus, W.; Guo, F.; Rocha, K.; Kumaraswamy, S.; Boyapalle, S.; Atadja, P.; Seto E.; Bhalla, K. Inhibition of histone deacetylase 6 acetylates and disrupts the chaperone function of heat shock protein 90. *J. Biol Chem*. **2005**, *280*, 26729-26734. c) Rao R.; Fiskus W.; Yang Y.; Lee P.; Joshi R.; Fernandez P.; Mandawat A.; Atadja P.; Bradner J. E.; Bhalla K. HDAC6 inhibition enhances 17-AAG mediated abrogation of Hsp90 chaperone function in human leukemia cells. *Blood*. **2008**, *112,* 1886-1893.

TOC Graphic